COMILLAS
UNIVERSIDAD PONTIFICIA
ICAI

MÁSTER UNIVERSITARIO EN INGENIERÍA INDUSTRIAL

TRABAJO FIN DE MÁSTER

ALGORITMO DE AGC PARA UNA ZONA DE REGULACIÓN CON SOLO GENERACIÓN RENOVABLE

Autor: Natalia de Frutos de la Torre

Director: Ignacio Egido Cortés

Co-Director: Ana Baringo Morales

Madrid

Agosto de 2025

Declaro, bajo mi responsabilidad, que el Proyecto presentado con el título

Algoritmo de AGC para una zona de regulación con solo generación renovable

en la ETS de Ingeniería - ICAI de la Universidad Pontificia Comillas en el

curso académico 2024/25 es de mi autoría, original e inédito y

no ha sido presentado con anterioridad a otros efectos.

El Proyecto no es plagio de otro, ni total ni parcialmente y la información que ha sido

tomada de otros documentos está debidamente referenciada.

Fdo.: Natalia de Frutos de la Torre Fecha: …25…/ …08…/ …2025…

Autorizada la entrega del proyecto

EL DIRECTOR DEL PROYECTO

Fdo.: Ignacio Egido Cortés Fecha: …25…/ …08…/ …2025…

MÁSTER UNIVERSITARIO EN INGENIERÍA INDUSTRIAL

TRABAJO FIN DE MÁSTER

ALGORITMO DE AGC PARA UNA ZONA DE REGULACIÓN CON SOLO GENERACIÓN RENOVABLE

Autor: Natalia de Frutos de la Torre

Director: Ignacio Egido Cortés

Co-Director: Ana Baringo Morales

Madrid

Acknowledgements

I would like to thank my supervisors for being there whenever I needed them, for their infinite patience and constant support, and for all the resources and guidance they provided. Their knowledge has been a great source of encouragement throughout this journey. They have guided me every step of the way and offered continuous feedback during the development of this project. Without their help, this work would not have been possible.

ALGORITMO DE AGC PARA UNA ZONA DE REGULACIÓN CON SOLO GENERACIÓN RENOVABLE

Autor: de Frutos de la Torre, Natalia
Director: Egido Cortés, Ignacio
Co-Director: Ana Baringo Morales
Entidad Colaboradora: ICAI – Universidad Pontificia Comillas

RESUMEN DEL PROYECTO

Este proyecto investiga la integración de un proveedor de servicios de balance totalmente renovable (BSP), compuesto por 30 parques eólicos, en la regulación secundaria de frecuencia mediante dos algoritmos AGC adaptados. El algoritmo de Despacho por Orden de Mérito (MO) maximiza el uso de energías renovables, pero introduce retrasos en la respuesta, mientras que el algoritmo de Banda de Regulación Proporcional (PRB) permite una regulación más rápida y equilibrada, aunque es sensible a las bandas muertas. Los resultados de las simulaciones demuestran la viabilidad técnica de los BSP eólicos para la regulación de frecuencia.

Palabras clave: AGC, energía eólica, aerogeneradores, regulación secundaria de frecuencia, BSP renovable

1. Introducción

La transición hacia un sistema energético sostenible y descarbonizado es uno de los principales retos del siglo XXI, impulsado por el creciente protagonismo de las fuentes de energía renovable. En España, más del 60 % de la capacidad instalada proviene de renovables, principalmente eólica (25,2 %) y solar fotovoltaica (20,8 %) [1]. Sin embargo, la variabilidad e imprevisibilidad inherentes a estos recursos plantean desafíos significativos para la estabilidad y fiabilidad del sistema eléctrico [2], [3].

La energía eólica se está consolidando rápidamente como una tecnología dominante a nivel mundial, aumentando progresivamente su participación en la generación eléctrica a medida que las fuentes renovables reemplazan a las centrales convencionales. En España, el cierre de las plantas de carbón y el plan de desmantelamiento de las centrales nucleares indican que los futuros Proveedores de Servicios de Balance (BSP) estarán compuestos predominantemente por unidades renovables. Tradicionalmente, las centrales convencionales aportaban la inercia mecánica esencial para la regulación de frecuencia, un servicio cuya ausencia quedó en evidencia durante el apagón ocurrido en abril de 2025 en España, lo que subraya la urgente necesidad de nuevas soluciones de inercia sintética.

Este proyecto aborda esa necesidad mediante el desarrollo de algoritmos que permiten a BSPs compuestos exclusivamente por parques eólicos participar de forma efectiva en la regulación de frecuencia. Ante el declive de la generación térmica y el auge de las renovables, es cada vez más necesario desarrollar soluciones tecnológicas que permitan a los aerogeneradores contribuir significativamente a los servicios de reserva secundaria. El objetivo principal es diseñar algoritmos de control que distribuyan de forma eficiente las consignas de potencia emitidas por el operador del sistema entre los distintos parques

eólicos, mejorando así el rendimiento de la regulación en línea con los nuevos requisitos del sistema.

2. Definición del proyecto

Estudios previos se han centrado en configuraciones híbridas que combinan unidades convencionales, renovables y sistemas de almacenamiento de energía en baterías (BESS). Este trabajo va un paso más allá al analizar un BSP compuesto exclusivamente por parques eólicos, concretamente 30 unidades, para evaluar su capacidad de proporcionar regulación secundaria dentro del sistema eléctrico español.

Investigaciones recientes han demostrado que los aerogeneradores, cuando se controlan adecuadamente, pueden igualar o incluso superar a las unidades convencionales en términos de respuesta de regulación [4]. Este estudio presenta dos algoritmos de regulación diseñados para optimizar el rendimiento técnico, limitar el desgaste mecánico y considerar los compromisos económicos asociados al mantenimiento de reservas [5].

Este trabajo evalúa el verdadero potencial individual de los parques eólicos para contribuir a la regulación secundaria de frecuencia bajo condiciones operativas reales mediante un algoritmo AGC adaptado. El estudio abarca el desarrollo e implementación del algoritmo en MATLAB y Simulink, simulaciones con datos reales de viento, evaluación del rendimiento conforme a los requisitos de regulación secundaria de Red Eléctrica de España (REE), y análisis de los resultados.

3. Descripción del modelo

El proyecto desarrollado en [6] fue modificado para excluir las unidades de generación convencionales. También se incorporó un nuevo modelo de evaluación de REE, incluyendo unidades no reguladoras. Las simulaciones se extendieron para cubrir períodos más largos y utilizar datos reales de generación que reflejan la máxima potencia disponible. Los algoritmos AGC originales se adaptaron a esta configuración totalmente renovable e implementaron en un bloque S-Function de Simulink que representa al BSP, el cual es el componente principal de este estudio. Una representación esquemática del modelo implementado se muestra en la Ilustración 1.

Los algoritmos de control están diseñados para distribuir la potencia de consigna recibida del Operador del Sistema entre los parques eólicos, considerando las restricciones técnicas y operativas de cada unidad para regular su salida. El objetivo es seguir con precisión la potencia de consigna del Operador del Sistema mientras se cumplen los criterios actualizados de evaluación de REE, permitiendo una evaluación técnica y económica integral. El desempeño del sistema se clasifica en cuatro categorías: Activo, Error, Alerta y Mala Respuesta (*Active, Error, Alert and Bad Response*), según la magnitud y duración de la desviación respecto al punto de referencia. Las desviaciones significativas y sostenidas en el tiempo (Mala Respuesta, *Bad Response*) implican penalizaciones económicas.

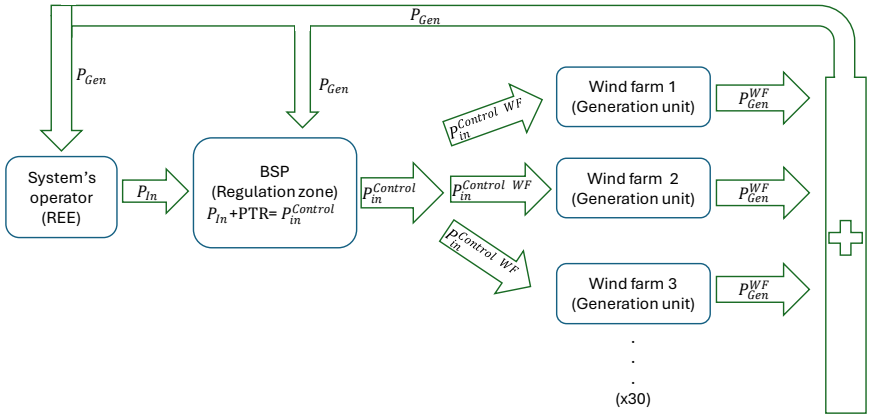

Ilustración 1. Operación esquemática del sistema

Los algoritmos desarrollados y sus características se explican a continuación:

Algoritmo de Despacho por Orden de Mérito

Este algoritmo distribuye la potencia de entrada según la capacidad máxima estimada de cada parque eólico. Inicialmente, todos los parques se configuran su potencia de consigna como la mínima estimada para asegurar una rápida capacidad de respuesta y reducir el desgaste mecánico. Luego, la potencia se asigna secuencialmente, comenzando por el primer parque eólico, hasta que la potencia a repartir se agote. La mayoría de los parques terminan saturados, mientras que el último recibe la potencia restante y los restantes, permanecen en el mínimo.

El algoritmo se ajusta para unidades no reguladoras (que producen independientemente) y desequilibrios del ciclo anterior. También considera la banda muerta de cada parque, modificando los puntos de consigna cuando los cambios pequeños quedan por debajo de este umbral, con un margen de ±0,5 MW para compensar imprecisiones.

Algoritmo de Banda de Regulación Proporcional

Este algoritmo distribuye la potencia de entrada proporcionalmente a la banda de regulación disponible de cada parque, definida como la diferencia entre sus límites de potencia estimados y el punto de consigna anterior. Esto evita la saturación y asegura una respuesta más rápida a las necesidades de regulación. Sin embargo, es sensible a los efectos de la banda muerta, que pueden bloquear pequeños cambios en la consigna de cada parque eólico.

Para solucionarlo, el algoritmo detecta los parques afectados y redistribuye la potencia bloqueada priorizando las unidades con bandas de regulación más amplias. Estas unidades reciben consignas ajustadas que superan la zona muerta en un 150%. Las unidades afectadas restantes mantienen su punto de consigna anterior si no queda potencia para distribuir.

Las unidades no reguladoras y aquellas sin banda de regulación se excluyen de la distribución, ya que su producción es predecible. A diferencia del algoritmo de Despacho

por Orden de Mérito (MO), aquí no se considera el desequilibrio de potencia del anterior ciclo para mantener la estabilidad.

4. Resultados

A continuación, se presentan los resultados de ambos algoritmos desarrollados. Para evaluar su desempeño, se seleccionó el perfil de potencia de entrada más exigente: una señal sinusoidal que oscila cerca de los niveles máximos y mínimos de potencia del sistema. Esto representa un desafío significativo para los algoritmos.

Algoritmo de Despacho por Orden de Mérito

La Ilustración 2 y la Ilustración 3 demuestran el buen desempeño del BSP, aunque se observa un retraso en la respuesta, principalmente causado por la presencia de parques eólicos no reguladores y la saturación de varias unidades reguladoras. Como resultado, los parques eólicos restantes deben absorber la mayor parte del esfuerzo de regulación, lo que ralentiza la respuesta general del sistema.

El retraso más notable ocurre en los picos positivos, donde el algoritmo sobreestima la disponibilidad de viento y establece puntos de consigna que superan lo físicamente alcanzable. Esta discrepancia solo se detecta en el ciclo de control siguiente, resultando en una leve demora al corregir la salida.

De manera similar, durante la presencia de unidades no reguladoras (de 10:00 a 12:00), el sistema no puede alcanzar los picos negativos debido a la insuficiente capacidad de regulación a la baja, ya que estas unidades permanecen fijas en su máxima potencia.

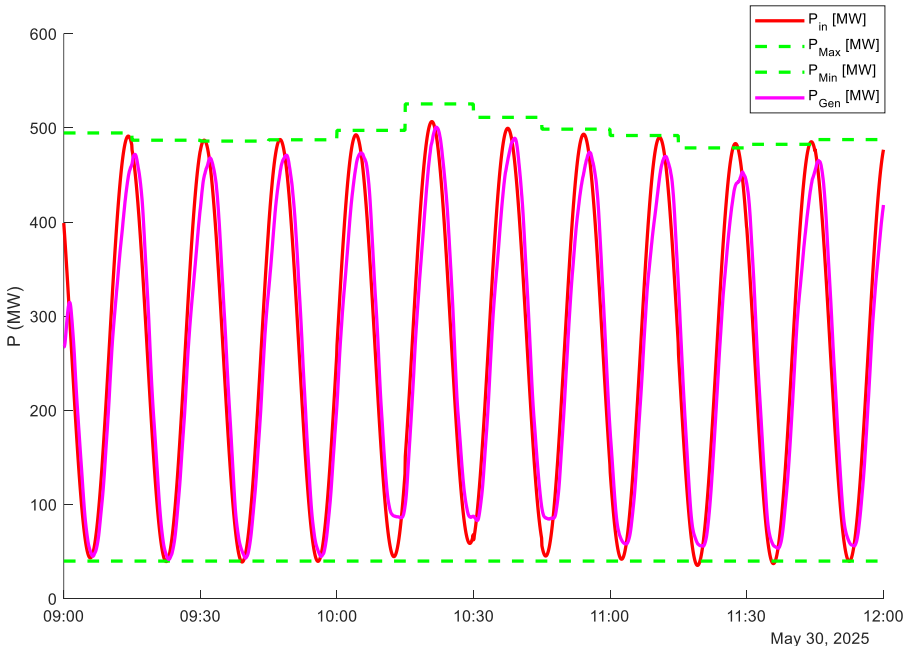

Ilustración 2. Resultados para la Señal Sinusoidal Cercana a la Potencia Máxima y Mínima Usando el Algoritmo MO

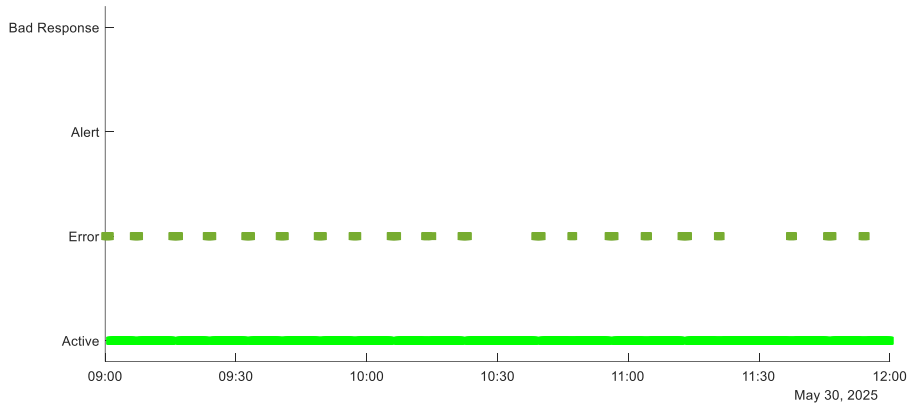

Ilustración 3. Evaluación del Desempeño para la Señal Sinusoidal Cercana a la Potencia Máxima y Mínima Usando el Algoritmo MO

Algoritmo de Banda de Regulación Proporcional

Los resultados demuestran que el algoritmo de Banda de Regulación Proporcional (PRB) funciona correctamente bajo condiciones de entrada altamente exigentes. Como se muestra en la Ilustración 4, la generación sigue de cerca la señal sinusoidal de consigna, excepto durante los picos, donde surgen limitaciones principalmente debido a la disponibilidad de viento (en los picos positivos) y al efecto de la banda muerta (en los picos negativos). En este último caso, el algoritmo no puede forzar a las unidades a operar por debajo de su mínimo técnico, por lo que persiste cierta desviación en los puntos más bajos.

Un pico positivo ocurre alrededor de las 10:20 a.m., donde la generación coincide completamente con la consigna debido a una mayor potencia máxima estimada y a una mayor disponibilidad de viento. En contraste, con el algoritmo MO, la generación se queda rezagada respecto a la consigna en los picos, ya que los grandes ajustes de generación impiden que la salida total alcance el máximo deseado.

La presencia de unidades no reguladoras limita aún más la capacidad de alcanzar los picos negativos, ya que no pueden reducir su producción.

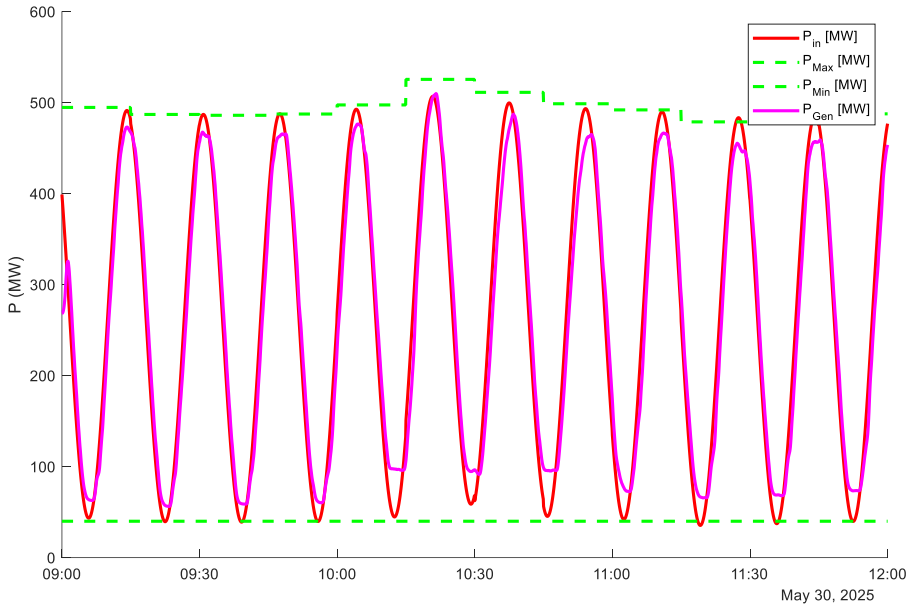

Ilustración 4. Resultados para la Señal Sinusoidal Cerca de la Potencia Máxima y Mínima Usando el Algoritmo PRB

La Ilustración 5 muestra la evaluación de este caso exigente: la mayoría de los resultados se sitúan dentro del área Activa. Solo se producen algunos errores, principalmente relacionados con las limitaciones de potencia mínima y las restricciones de las unidades no reguladoras. En general, este escenario confirma la robustez del algoritmo.

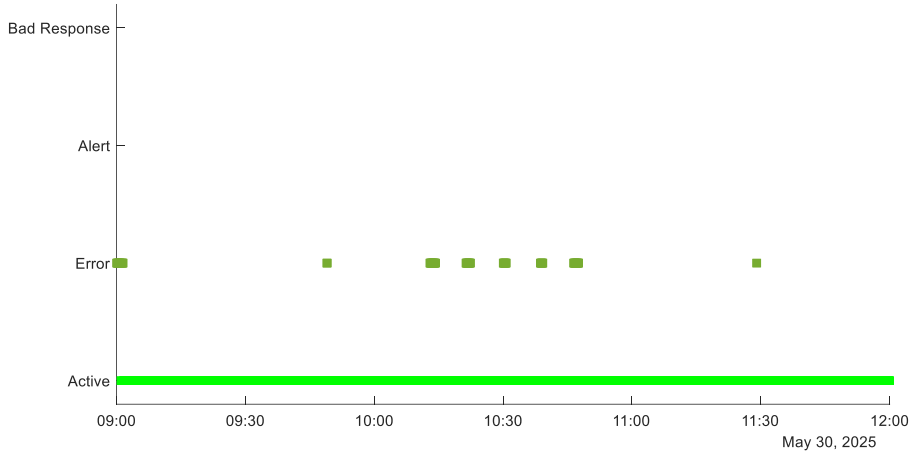

Ilustración 5. Evaluación del Desempeño para la Señal Sinusoidal Cerca de la Potencia Máxima y Mínima Usando el Algoritmo PRB

5. Conclusiones

El algoritmo MO maximiza el uso de la energía eólica, pero provoca una distribución de potencia desequilibrada entre las unidades, con algunas saturadas y otras inactivas. Esto genera retrasos en la respuesta y reduce la estabilidad, especialmente en condiciones de alta exigencia. Además, presenta un retraso de un ciclo cuando la consigna supera la potencia disponible. Finalmente, este algoritmo no es muy sensible a las bandas muertas ni a las unidades no reguladoras, ya que la mayoría de los parques eólicos operan a su

potencia máxima. Además, la potencia de salida del BSP es más estable en comparación con la del algoritmo PRB.

En cambio, el algoritmo PRB distribuye la potencia de manera más equilibrada según el rango de regulación de cada unidad. Esto mejora la capacidad de respuesta y el aprovechamiento de los activos, aunque su rendimiento se ve afectado por las bandas muertas y la presencia de unidades no reguladoras, lo que en ocasiones provoca fluctuaciones al compensar pequeños cambios en la consigna.

A pesar de estas limitaciones, ambos algoritmos cumplen con los objetivos del proyecto, demostrando que los parques eólicos pueden participar eficazmente en la regulación secundaria de frecuencia mediante estrategias de control.

6. Referencias

[1] 'Potencia instalada | Informes del sistema'. Consultado: Mar. 23, 2025. [Online]. Disponible: https://www.sistemaelectrico-ree.es/informe-del-sistema-electrico/potencia-instalada.

[2] K. De Vos and J. Driesen, 'Balancing management mechanisms for intermittent power sources — A case study for wind power in Belgium', in 2009 6th International Conference on the European Energy Market, May 2009, pp. 1–6. doi: 10.1109/EEM.2009.5207190.

[3] A. Gonzalez-Garrido, A. Saez-de-Ibarra, H. Gaztanaga, A. Milo, and P. Eguia, 'Annual Optimized Bidding and Operation Strategy in Energy and Secondary Reserve Markets for Solar Plants With Storage Systems', IEEE Trans. Power Syst., vol. 34, no. 6, pp. 5115–5124, Nov. 2019, doi: 10.1109/TPWRS.2018.2869626.

[4] T. Sow, O. Akhrif, A. F. Okou, A. O. Ba, and R. Gagnon, 'Control strategy insuring contribution of DFIG-Based wind turbines to primary and secondary frequency regulation', in IECON 2011 - 37th Annual Conference of the IEEE Industrial Electronics Society, Melbourne, Vic, Australia: IEEE, Nov. 2011, pp. 3123–3128. doi: 10.1109/IECON.2011.6119809.

[5] K. D. Vos, P. S. Perez, and J. Driesen, 'The Participation in Ancillary Services by High Capacity Wind Power Plants: Reserve Power'.

[6] N. de Frutos de la Torre, 'Mejora de un algoritmo de AGC para la integración de parques eólicos en regulación', 2023.

AGC ALGORITHM FOR A CONTROL AREA WITH ONLY RENEWABLE GENERATION

Author: de Frutos de la Torre, Natalia
Supervisor: Egido Cortés, Ignacio
Co-Supervisor: Ana Baringo Morales
Collaborating Entity: ICAI – Universidad Pontificia Comillas

ABSTRACT

This project investigates the integration of a fully renewable Balancing Service Provider (BSP) of 30 wind farms into secondary frequency regulation using two adapted AGC algorithms. The Merit Order Algorithm maximises renewable utilisation but introduces response delays, while the Proportional Regulation Band Algorithm enables faster, more balanced regulation but is sensitive to deadbands. Simulation results demonstrate the technical feasibility of wind-based BSPs for frequency regulation.

Keywords: AGC, wind energy, wind turbines, secondary frequency regulation, renewable BSP

1. Introduction

The transition towards a sustainable and decarbonised energy system is one of the major challenges of the 21st century, driven by the increasing share of renewable energy sources. In Spain, over 60% of installed capacity comes from renewables, mainly wind (25.2%) and solar PV (20.8%) [1]. However, the inherent variability and unpredictability of these resources pose significant challenges to grid stability and reliability [2], [3].

Wind power is rapidly becoming a dominant technology worldwide, steadily increasing its contribution to electricity generation as renewable sources gradually replace conventional power plants. In Spain, the retirement of coal-fired plants and the planned decommissioning of nuclear stations indicate that future Balancing Service Providers (BSPs) will be predominantly composed of renewable units. Traditionally, conventional plants provided mechanical inertia crucial for frequency regulation, a service whose absence was evident during the Spanish blackout of April 2025, highlighting the urgent need for new synthetic inertia solutions.

This project addresses this gap by developing algorithms that enable BSPs made up exclusively of wind farms to participate effectively in frequency regulation. With thermal generation declining and renewables rising, there is an increasing necessity for technological advancements that allow wind turbines to contribute meaningfully to secondary reserve services. The main goal is to design control algorithms that efficiently distribute power setpoints issued by the System Operator among the wind farms, improving regulation performance in accordance with evolving system requirements.

2. Project Definition

Previous studies have focused on hybrid configurations combining conventional, renewable units, and Battery Energy Storage Systems (BESS). This work advances the field by analysing a BSP composed entirely of wind farms, specifically 30 units, to assess its capability to provide secondary regulation within the Spanish power system.

Recent research has shown that wind turbines, when appropriately controlled, can match or even surpass conventional units in terms of regulation response [4]. This study introduces two regulation algorithms designed to optimise technical performance, limit mechanical wear, and account for economic trade-offs associated with maintaining reserves [5].

This work evaluates the true individual potential of wind farms to contribute to secondary frequency regulation under real operating conditions through a tailored AGC algorithm. The study involves developing and implementing the algorithm in MATLAB and Simulink, simulating with real wind data, assessing performance according to Red Eléctrica de España (REE) secondary regulation requirements, and analysing the results.

3. System description

The project developed in [6] was modified to exclude conventional generation units. A new REE evaluation model was also incorporated and include non-regulating units. Simulations were extended to cover longer periods and use actual generation data that reflect the maximum available power. The original AGC algorithms were adapted to this fully renewable configuration and implemented in a Simulink S-Function block representing the BSP, which is the main component of this study. A schematic representation of the implemented model is shown in Illustration 1.

The control algorithms are designed to distribute the power setpoint received from the System Operator among the wind farms, considering each unit's technical and operational constraints to regulate their output. The objective is to accurately track the setpoint while meeting REE's updated performance criteria, enabling a comprehensive technical and economic evaluation. System performance is classified into four categories, Active, Error, Alert, and Bad Response, based on the magnitude and duration of deviation from the setpoint. Significant and sustained deviations (Bad Response) result in economic penalties.

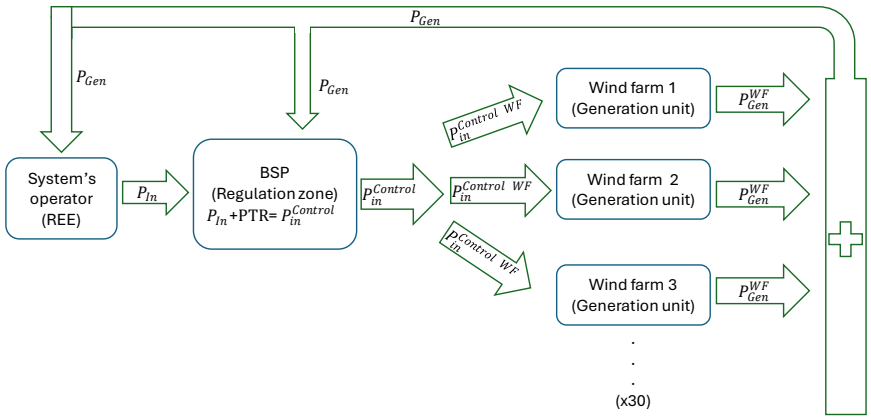

Illustration 1. Schematic Operation of the System

The developed algorithms and their characteristics are explained below:

Merit Order Algorithm

This algorithm distributes input power based on each wind farm's estimated maximum capacity. All farms are initially set to their minimum output to ensure rapid response capability and reduce mechanical wear. Then, power is allocated sequentially, starting from the first wind farm, until the available input power is exhausted. Most WFs end up saturated, while the last receives the remaining power and others remains at minimum output.

The algorithm adjusts for non-regulating units (which produce independently) and previous cycle imbalances. It also considers each WF's deadband, modifying setpoints when small changes fall below this threshold, with a ±0.5 MW buffer to account for inaccuracies.

Proportional Regulation Band Algorithm

This algorithm distributes input power proportionally to each WF's available regulation band, the difference between its estimated power limits and previous setpoint. This prevents saturation and ensures quicker response to regulation needs. However, it is sensitive to deadband effects, which can block small setpoint changes.

To address this, the algorithm detects affected WFs and redistributes the blocked power by prioritising units with larger regulation bands. These units receive adjusted setpoints exceeding the deadband by 150%. Remaining affected units retain their previous setpoint if no power remains.

Non-regulating units and those with no regulation band are excluded from the distribution, as their output is predictable. Unlike the Merit Order (MO) algorithm, past power imbalance is not considered here to maintain stability.

4. Results

Below are the results for both developed algorithms. To evaluate their performance, the most demanding input power profile was selected: a sinusoidal signal oscillating near the system's maximum and minimum power levels. It presents a significant challenge for the algorithms.

Merit Order Algorithm

Illustration 2 and Illustration 3 demonstrate the strong performance of the BSP response delay is observed, mainly caused by the presence of non-regulating wind farms and the saturation of several regulating units. As a result, the remaining wind farms must absorb most of the regulation effort, which slows down the system's overall response. The most noticeable delay occurs at the positive peaks, where the algorithm overestimates wind availability and sets setpoints beyond what is physically achievable. This mismatch is only detected in the subsequent control cycle, resulting in a slight lag when correcting the output.

Similarly, during the presence of non-regulating units (from 10:00 to 12:00), the system is unable to reach the negative peaks due to insufficient downward regulation capacity, as these units remain fixed at maximum output.

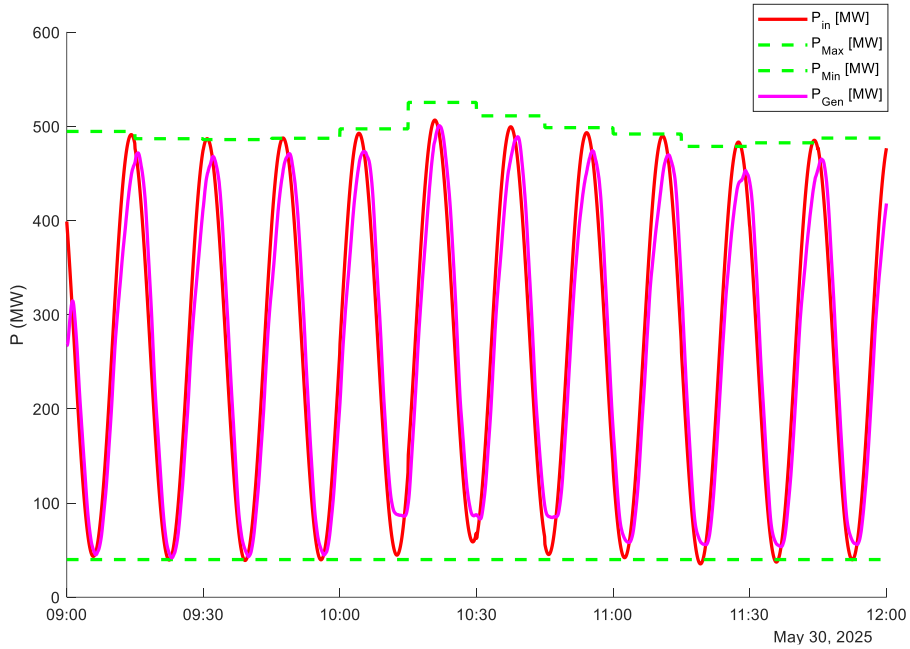

Illustration 2. Results for the Sinusoidal Signal Near the Maximum and Minimum Power Using the MO Algorithm

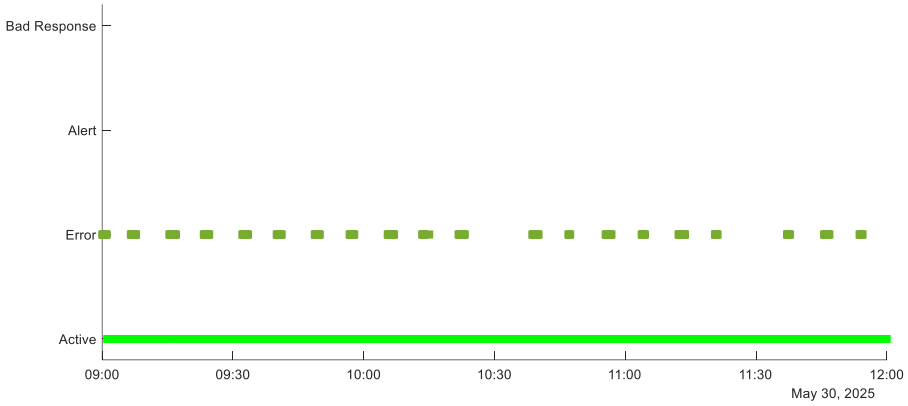

Illustration 3. Performance Evaluation for the Sinusoidal Signal Near the Maximum and Minimum Power Using the MO Algorithm

Proportional Regulation Band Algorithm

The results demonstrate that the Proportional Regulation Band (PRB) algorithm performs well under highly demanding input conditions. As shown in Illustration 4, generation closely tracks the sinusoidal setpoint, except during peaks where limitations arise, mainly due to wind availability (at positive peaks) and the deadband (at negative peaks). In the latter case, the algorithm cannot force units below their technical minimum, so some deviation remains at the lowest points.

A notable positive peak occurs around 10:20 a.m., where the generation fully matches the setpoint due to higher estimated maximum power and increased wind availability. In contrast, with the MO algorithm, generation lags behind the setpoint at peaks because large adjustments prevent the total output from reaching the desired maximum

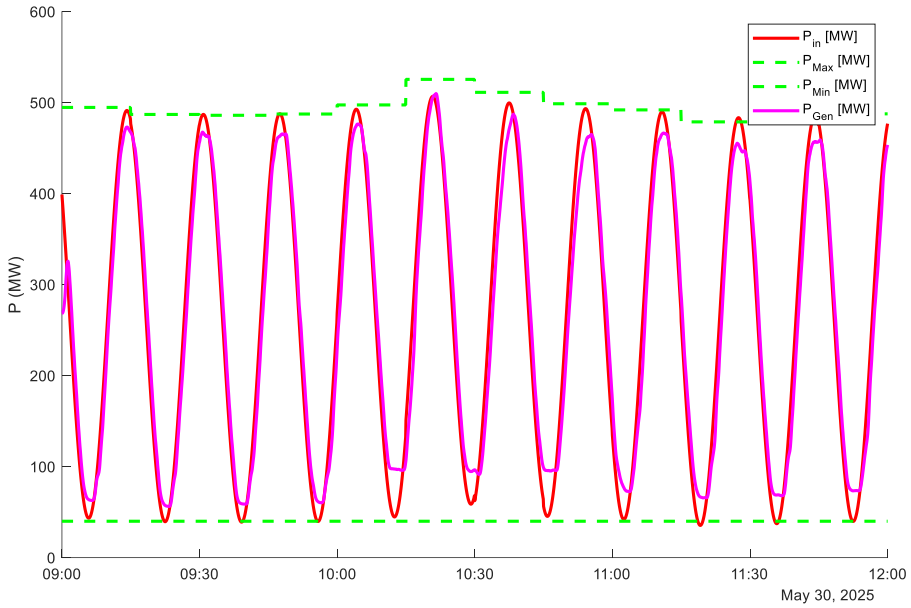

Illustration 4. Results for the Sinusoidal Signal Near the Maximum and Minimum Power Using the PRB Algorithm

The presence of non-regulating units further restricts the ability to reach negative peaks, as they cannot reduce output. Illustration 5 shows the evaluation of this challenging case: most results fall within the *Active* area. Only a few errors occur, primarily linked to minimum power limitations and non-regulating unit constraints. Overall, this scenario confirms the robustness of the algorithm.

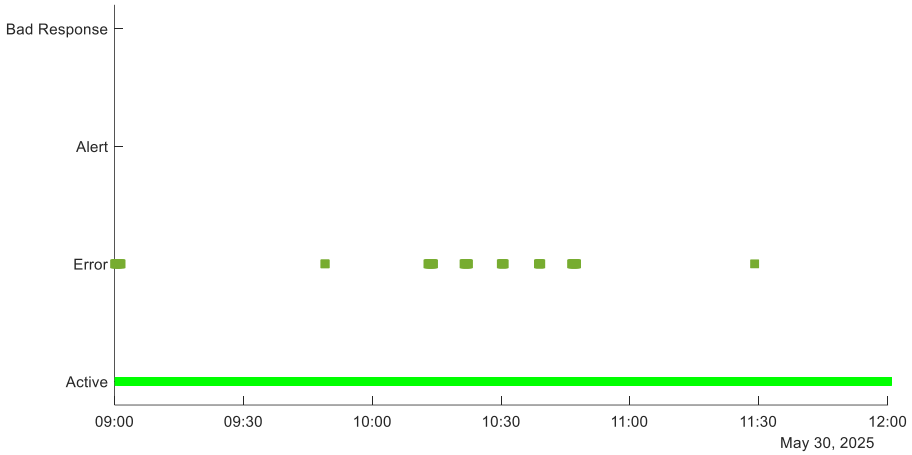

Illustration 5. Performance Evaluation for the Sinusoidal Signal Near the Maximum and Minimum Power Using the PRB Algorithm

5. Conclusions

The MO algorithm maximises wind power use but results in an unbalanced workload across units, with some becoming saturated and others remaining idle. This leads to delayed responses and reduced stability, particularly under high-demand conditions. It also reacts with a one-cycle delay when the setpoint exceeds the available power. Finally, this algorithm is not affected by deadbands or non-regulating units, as most of the wind

farms operate at their maximum output. Additionally, the BSP's output power is smoother compared to that of the PRB Algorithm.

In contrast, the PRB algorithm distributes power more evenly based on each unit's regulation range. This improves responsiveness and asset utilisation, but its performance is affected by deadbands and non-regulating units, sometimes causing output fluctuations when compensating for small setpoint changes.

Despite these limitations, both algorithms achieved the project's objectives, demonstrating that wind farms can effectively participate in secondary frequency regulation using customised control strategies.

6. References

[1] 'Potencia instalada | Informes del sistema'. Accessed: Mar. 23, 2025. [Online]. Available: https://www.sistemaelectrico-ree.es/informe-del-sistema-electrico/potencia-instalada.

[2] K. De Vos and J. Driesen, 'Balancing management mechanisms for intermittent power sources — A case study for wind power in Belgium', in *2009 6th International Conference on the European Energy Market*, May 2009, pp. 1–6. doi: 10.1109/EEM.2009.5207190.

[3] A. Gonzalez-Garrido, A. Saez-de-Ibarra, H. Gaztanaga, A. Milo, and P. Eguia, 'Annual Optimized Bidding and Operation Strategy in Energy and Secondary Reserve Markets for Solar Plants With Storage Systems', *IEEE Trans. Power Syst.*, vol. 34, no. 6, pp. 5115–5124, Nov. 2019, doi: 10.1109/TPWRS.2018.2869626.

[4] T. Sow, O. Akhrif, A. F. Okou, A. O. Ba, and R. Gagnon, 'Control strategy insuring contribution of DFIG-Based wind turbines to primary and secondary frequency regulation', in *IECON 2011 - 37th Annual Conference of the IEEE Industrial Electronics Society*, Melbourne, Vic, Australia: IEEE, Nov. 2011, pp. 3123–3128. doi: 10.1109/IECON.2011.6119809.

[5] K. D. Vos, P. S. Perez, and J. Driesen, 'The Participation in Ancillary Services by High Capacity Wind Power Plants: Reserve Power'.

[6] N. de Frutos de la Torre, 'Mejora de un algoritmo de AGC para la integración de parques eólicos en regulación', 2023.

Nomenclature

P_{Gen}	Generated Power TOTAL	MW
P_{Gen}^{WF}	Wind Farm Generated Power	MW
P_{Gen}^{CU}	Conventional Unit Generated Power	MW
P_{In}	Dispatch power (System Operator (SO)) TOTAL	MW
$P_{in}^{Control}$	Dispatch Power (control) TOTAL	MW
$P_{in}^{Control\ PC}$	Previous Cycle Dispatch Power (control) TOTAL	MW
$P_{in}^{Control\ WF}$	Wind Farm Dispatch Power (control)	MW
$P_{in}^{Control\ WF\ PC}$	Previous Cycle Wind Farm Dispatch Power (control)	MW
$P_{in}^{Control\ TWF}$	TOTAL Dispatch Power of Wind Farms (control)	MW
$P_{in}^{Control\ TWF\ PC}$	Previous Cycle Total Dispatch Power of Wind Farms (control)	MW
$P_{in}^{Control\ CU}$	Conventional Unit Dispatch Power (control)	MW
P_{Max}	Maximum Estimated Power TOTAL	MW
P_{Max}^{WF}	Wind Farm Maximum Estimated Power	MW
P_{Min}	Minimum Estimated Power TOTAL	MW
P_{Min}^{WF}	Wind Farm Minimum Estimated Power	MW
P_{Real}^{WF}	Wind Farm Real Power	MW
PTR	BSP Scheduled Power	MW
CRR	Dispatch power (SO – Global AGC) TOTAL	MW

Contents

List of Figures

Chapter 1. INTRODUCTION

The transition towards a sustainable and decarbonised energy system represents one of the greatest challenges of the 21st century. In this context, renewable energy sources are playing an increasingly significant role in power grids worldwide, driven by environmental policies, technological advancements, and growing societal awareness of climate change.

This trend is particularly evident in the Spanish electrical grid, where 61.3% of the installed capacity comes from renewable sources in 2024, mainly wind (25.2%) and photovoltaic (PV) solar energy (20.8%) [1]. Globally, countries such as the United States are also advancing in this direction; the U.S. Department of Energy projects that by 2030, 20% of the electricity generated will come from renewable sources [2].

However, the growing integration of these technologies presents major technical challenges. In contrast to conventional power sources that can be dispatched on demand, renewable energies exhibit inherent variability, lower predictability, and difficult to control [3] due to their reliance on weather patterns and geographic location. This variability directly affects the energy balance of the system, thereby compromising the stability and reliability of the electrical grid [4].

As renewable power penetration increases, grid imbalances become more frequent and severe [5]. A clear example of this vulnerability occurred on 28th April 2025, during the largest blackout in European history. This event underscored the difficulties of renewable integration and the urgent need for effective frequency regulation mechanisms [6]. At the time of the incident, Spain's electricity mix consisted of 60.64% solar PV, 12% wind, and 11.6% nuclear [7]. At 12:33 p.m., two grid disturbances in southern Spain led to a critical drop in system frequency below 50 Hz. Two minutes later, France was disconnected, resulting in the collapse of a significant portion of the interconnected European grid [6], [7]. The incident exposed the grid's susceptibility to instability caused by low system inertia, which stems directly from the high share of renewable energy [6].

This work focuses on enabling wind farms to contribute to secondary reserve services in Spain. Although the size of wind farms in countries like Spain and the United Kingdom is sufficient to provide reserve services, their current participation remains limited, primarily due to economic constraints [8].

Despite the increased penetration of wind energy, the cost of secondary reserve services has not risen [9]. However, the need for these services is growing, due to the reduction in thermal generation and the expansion of renewable sources. Therefore, it is urgent to develop effective technological solutions that enable wind turbines to contribute to frequency regulation.

The main objective of this project is to develop a proposal that enables the efficient and unrestricted integration of wind technologies into secondary reserve services. This represents a key step toward achieving a fully green and sustainable power grid.

The structure of this work is: the initial chapters provide background information and a review of the existing literature, followed by a detailed explanation of the project definition, methodology, and a comprehensive description of the developed algorithms and model. The results are then presented and discussed, and the document concludes with a summary of the key findings and recommendations for future work.
The main objectives of this project are: to design algorithms that distribute the power stipulated by the System Operator among the power generation units; and to evaluate their performance in accordance with the new System Operator's Regulation Service.

Chapter 2. LITERATURE REVIEW

The integration of wind turbines into secondary frequency regulation remains insufficiently addressed in the literature [10]. Prior work in [11] developed two Automatic Generation Control (AGC) algorithms for a Balancing Service Provider (BSP) comprising seven conventional units and one renewable unit. The present study extends this framework to a BSP composed exclusively of renewable sources. Specifically, up to 30 wind farms, have been used to evaluate their suitability for secondary regulation within the Spanish power system.

Several studies highlight the technical potential of wind turbines in AGC. As shown in [12], wind turbines can achieve response times comparable to, or exceeding, those of thermal units when equipped with droop control and supplementary pitch angle control loops. Moreover, [13] demonstrated that curtailing turbine output by 20% and increasing rotor speed enhances reserve provision and system flexibility. This principle underpins the algorithms introduced here, which reserves operational headroom by intentionally limiting wind farms from operating at full capacity.

Some papers, such as [14], have developed various technical strategies to incorporate wind turbines into secondary control. In particular, the solution proposed in [14] focuses on addressing wind variability, which is one of the main challenges for wind turbine integration. Reference [15] presents a literature review summarising current technical strategies across different inertia systems, wind-speed variations, and operational scenarios. It demonstrates that hybrid systems, such as combinations of wind turbines with battery energy storage systems (BESS) or conventional units, provide superior inertia control compared to traditional approaches, particularly during low-frequency events. However, in this project the wind farms are used without any storage system, trying to demonstrate that storage, although helpful, is not necessary for AGC provision by windfarms.

Building on this idea, several studies have also explored control allocation strategies within these hybrid systems. In [16], a configuration combining wind turbines, conventional units, and BESS showed that equal distribution of control effort reduces energy costs. Although the present work excludes BESS, it adopts a similar control logic to ensure wind turbines remain within technical output limits, improving regulation efficiency. In [17], a system comprising wind farms and BESS is proposed, under the premise that wind turbines alone lack sufficient rotor kinetic energy to provide primary control. To address this, a coordinated control strategy is implemented to manage frequency deviations, with BESS prioritized due to their faster response capabilities. Again, as this project is focused on secondary regulation, it is conducted using only wind turbines to assess the feasibility of their integration into a regulation zone without the need of additional storage systems.

Wind turbines can be combined not only with BESS, but also with concentrated solar power (CSP) plants, as shown in [18]. This study demonstrates that such a hybrid configuration provides better frequency control response than conventional thermal power plants and, economically, leads to increased revenue.

Mechanical reliability is another critical aspect. Frequent pitch angle adjustments can accelerate component wear, as noted in [13] and [19]. One of the proposed algorithms in this project mitigates this issue by avoiding large, rapid fluctuations in control signals, thereby reducing mechanical stress.

Economic considerations are equally relevant. According to [20], maintaining upward reserve may result in foregone market revenue and green certificate opportunities, while downward reserve does not incur comparable costs. This trade-off is incorporated in this project into the algorithm design to ensure economic as well as technical feasibility.

Forecast uncertainty and system flexibility are addressed in [21], which proposes pooling wind and conventional units alongside a backup generator sized to the largest contributor. A similar principle guides the Merit Order Algorithm developed here, wherein non-regulating wind farms act as reserve providers once others reach saturation. This approach aligns with

findings in [12], [22], [23], [24], underscore the need for dedicated reserves to maintain frequency stability under high renewable penetration.

Chapter 3. DEFINITION OF THE PROJECT

3.1 JUSTIFICATION

As demonstrated in the previous chapters (Chapter 1. and Chapter 2.), wind power is becoming one of the most important technologies in power systems worldwide. The share of electricity generated by wind farms continues to grow each year, consolidating their role as a vital component of both present and future energy systems. Among renewable energy sources, wind power is currently the most widely installed technology.

Renewable sources are progressively replacing conventional generation units. In Spain, for example, coal-fired power plants have been shut down, and nuclear power stations are scheduled for decommissioning at the end of their operational lifespans. Currently some BSPs consist solely of renewable energy units and this will probably apply to many of them in the near future.

To the best of the author of the project knowledge, no Automatic Generation Control (AGC) algorithm has been previously designed specially focused to manage a BSP composed entirely of renewable energy sources. However, this scenario is increasingly common and represents the direction in which power systems are evolving. The algorithms proposed in this study fully utilise the available wind power, maximising energy output and, therefore, economic returns.

The solutions developed in this work are novel and specifically designed to enable frequency regulation in BSPs composed exclusively of wind farms. They contribute directly to the goals of energy transition and power system decarbonisation, while ensuring optimal economic performance at all times.

3.2 OBJECTIVES

The ultimate goal of this project is the integration of control areas composed exclusively of renewable units—such as wind farms—into the secondary frequency regulation of the power system through an Automatic Generation Control (AGC) algorithm. To achieve this objective, the following specific goals must be accomplished:

- Develop a regulation algorithm that determines the power output of the different renewable units in the control area based on the setpoint provided by the System Operator.
- Implement the algorithm in a control area simulated using Matlab and Simulink.
- Simulate the algorithm within the control area using real generation data from wind units.
- Evaluate the system response according to the new Secondary Regulation Service requirements of Red Eléctrica de España (REE).
- Analyse the results obtained from the various simulations.

3.3 METHODOLOGY

To carry out this project, it is necessary to begin by modifying a previous model [11], which will serve as the basis for the various simulations. This model originates from an earlier project in which different AGC algorithms were developed to regulate a control area composed of both wind and conventional units. For the purposes of this project, the conventional units, the area controller from that project, and the performance indicators (KPIs) used in its evaluation are removed.

Additionally, a new response evaluation model developed by Red Eléctrica de España (REE) is introduced. This model not only assesses the technical performance but also establishes the economic incentives and penalties applied in case of non-compliance with the System

Operator's setpoints. As a result, this project also incorporates an economic analysis. Furthermore, the previously used algorithms are retained and improved.

Another significant difference from the previous project is the extension of the simulation period, which was previously limited to one hour, as well as the adaptation to the new AGC economic and technical procedure (SRS) that was released in Spain by REE (the Spanish System Operator) in November 2024.

A thorough literature review has been conducted to explore various models and case studies that help to better understand the specific challenges and characteristics of the topic. This research will also serve as a valuable source for identifying applicable solutions for the project's development.

Once the model has been adapted and the challenges and possible solutions are well understood, the different algorithms have been modified accordingly. The model has been simulated using real data on nominal power and actual wind generation, recorded over a specific period. Since the generation data was collected during a time when the units were not under regulation, it reflects the maximum achievable power under the given meteorological conditions.

Another key input to the model is the power setpoint to be regulated by the control area, provided by the System Operator and referred to as the automatic Frequency Restoration Reserve Setpoint (PaFRRSet). This input is processed by the algorithm, which determines the power setpoint for each unit. Using the response models of the units, the generation response of each one is obtained in the model.

Subsequently, the performance of each control algorithm is evaluated based on the criteria established by REE. This enables a realistic assessment of the behaviour of the BSP under the control of each proposed algorithm, allowing for a comprehensive evaluation of their technical and economic impact on the control area.

3.4 PLANNING AND ECONOMIC ESTIMATION

The organisation and timeline followed in this project are detailed below:

1. Modify previous algorithms and system: until 12th December 2024
2. Make a literature review: until 17th March 2025
3. Develop the algorithms: until 20th February 2025
4. Simulate the algorithms: until 9th April 2025
5. Evaluate the algorithms: until 17th May 2025
6. Write MSc tesis: until 30th June 2025

The economic estimation of the project considers the following expenses:

- Software license costs:
    - Microsoft 365 Personal: €99
    - MATLAB: €938
- Personnel cost:
    - Total hours: 360 (based on 12 ECTS credits)
    - Average hourly rate for a newly graduated engineer from the ICAI School of Engineering, according to the National College of ICAI Engineers: €15/hour
    - Total: €5,400

Total estimated cost of the project: €6,437

Chapter 4. DEVELOPED MODEL

This project models and simulates a BSP (Balancing Service Provider) composed of a single BSP integrating up to 30 wind farms within the Spanish power system. To achieve this, the model was developed in MATLAB and Simulink, using real input data. Specifically, a 24-hour recording of output power from 30 non-regulating wind farms was used, representing the maximum available power throughout that day. Additionally, the rated power of each wind farm was included in the model.

4.1 FREQUENCY REGULATION OPERATION

It is important to keep the grid frequency stable at its nominal value—50 Hz in Spain—to ensure the proper operation of generators and motors [20]. To achieve this, generation and demand must be balanced at all times. Any deviation will trigger the activation of reserve power, which is typically provided by adjusting the operating point of a power plant, energy storage systems, or controllable loads [20]. These actions fall under the scope of Ancillary Services, which include frequency regulation and are defined in [25] as "grid support services required by the transmission or distribution system operator to maintain the integrity and stability of the transmission or distribution system as well as the power quality. These services typically include regulation of frequency, active power reserves, voltage and reactive power control, black start capability and islanding". In the Spanish electricity market, a regulatory change in 2016 enabled renewable energy sources to participate in ancillary services, opening the door to their involvement in frequency regulation and other system support tasks [26]. Within this framework, Automatic Generation Control (AGC) plays a key role, initiating its operation once the primary frequency control has completed its immediate response.

Primary frequency control balances generation and demand by correcting power imbalances in the system to prevent large frequency deviations [27]. This control stabilises the frequency

at a value different from the nominal one, with generating units adjusting their output by approximately 1.5% of their rated power within 15 to 30 seconds [27].

Secondary control, also known as AGC, activates around 20 to 30 seconds after the initial imbalance, once the primary control response concludes. Its function is to restore both the system frequency and the scheduled power interchange to their nominal values [27]. In Spain, the power system is considered a single control area, which is subdivided into several zones (called BSP), each formed by a group of generating units [27]. In this project, only one BSP is considered, composed of up to 30 wind farms cooperating to achieve the desired behaviour of the regulating zone.

The System Operator determines the required power adjustment based on the results of a real time market where the different BSP bid to participate in AGC [28]. Each BSP receives a regulation signal, which is then distributed among the units according to technical and economic constraints [27]. The System Operator also evaluates the performance of each BSP and may impose financial penalties if the response does not meet established criteria [28].

Following AGC, tertiary control is initiated to restore generating units secondary reserve and release them from their secondary reserve commitments. The duration of tertiary control ranges from 15 minutes to 2 hours [27].

4.2 INITIAL SYSTEM

This project builds upon an Automatic Generation Control (AGC) algorithm developed in a previous study [11], which required several modifications. The original system model consisted of eight generation units: seven conventional units and one wind unit, under the framework of the previous AGC procedure in the Spanish power system, known as RCP (Regulación Compartida Peninsular). A schematic representation of the simulated model is shown in Figure 1. The system receives an AGC setpoint, known as the Required Regulation Power (CRR) [29], determined by the System Operator for each regulation zone. This dispatch signal is calculated by the Shared Peninsular Regulation (RCP)—which refers to

the Spanish System Operator, *Red Eléctrica de España* (REE)—using the Area Control Error (ACE) [29].

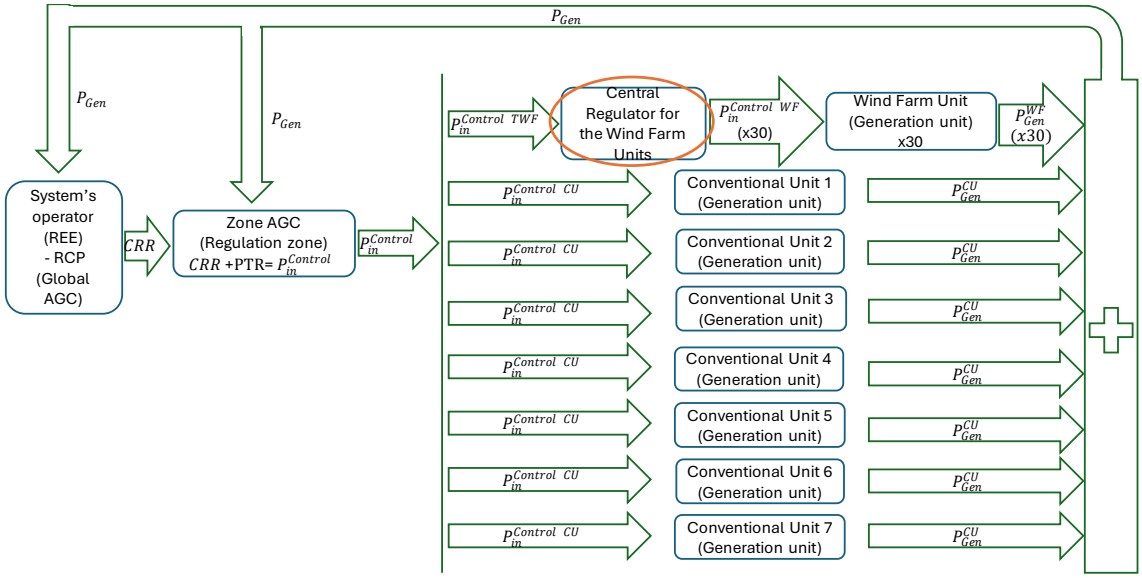

Figure 1. Schematic Operation of the Initial System

Since the project focuses on frequency regulation within the Spanish power system, REE is the operator responsible for this function. The ACE is computed for the entire country, taking into account the deviation between scheduled and generated power, the frequency deviation, and the real-time CRR [29]. The AGC setpoint (CRR) is then combined with the power scheduled in the day-ahead energy market, as was the procedure under the previous Spanish AGC regulation framework [29].

In the Simulink model (see in Figure 1), the *Zone AGC* block distributes the total setpoint power among the generation units. Within the wind farm unit, the *Wind Farm Unit* block simulates the operation of wind generation (representing the 30 individual wind farms) and is coordinated by the *Central Regulator for the Wind Farm Units* block (highlighted with an orange circle in Figure 1). This block is implemented as a S-Function in Simulink, where

various AGC algorithms previously developed in [11] are integrated. Its role is to distribute the unit-level setpoint among the 30 wind farms, considering their technical limitations, and ensuring compliance with BSP operational requirements.

4.3 CURRENT SYSTEM

The initial system described in [11] was modified to the configuration shown in Figure 2, which presents a schematic diagram illustrating the operation of the entire system. The conventional units, as well as the *Zone AGC* block from Figure 1, were removed. In this project, the system represents a AGC zone (BSP) composed of up to 30 wind farms. No conventional unit is included in the BSP.

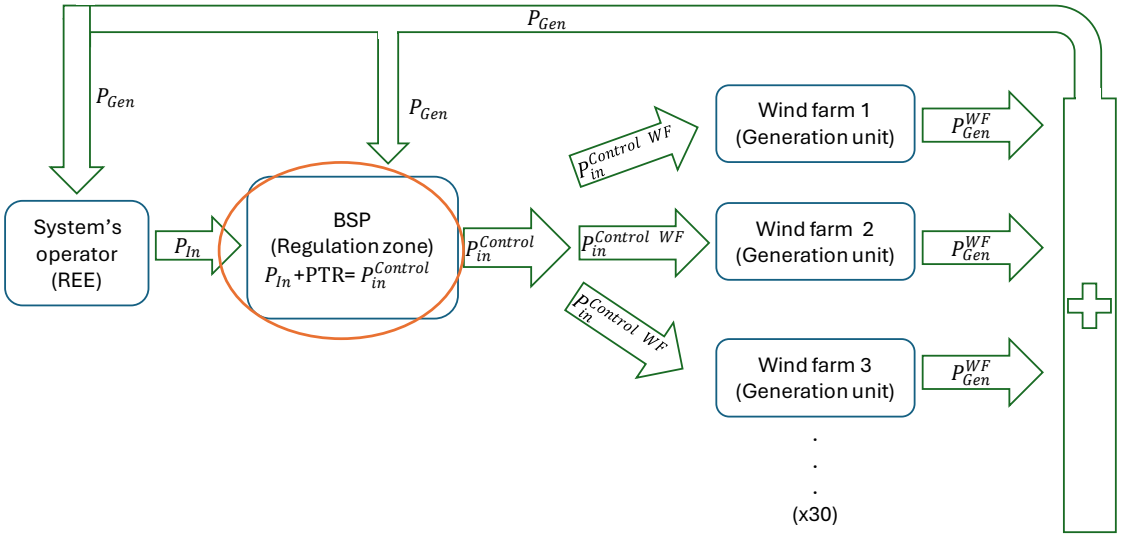

Figure 2. Schematic Operation of the Current System

The algorithms developed in the previous project (explained in 4.5) were adapted to accommodate the exclusive presence of renewable generators and implemented within the Simulink S-Function block *BSP (Regulation zone)* (highlighted with an orange circle in

Figure 2). This component is the primary focus of the current project, as all development and integration efforts were conducted within it.

The implemented algorithms are responsible for distributing the setpoint power provided by the System Operator among the wind farms, considering their technical constraints, operational characteristics, and possible limitations. The objective is to ensure that the total generated power closely tracks the setpoint assigned by REE.

The wind model, represented by the *Wind Farm Unit* block, follows the schematic shown in Figure 3. This model remains unchanged from the original system in [11] and represents the main dynamics of a single windfarm from the setpoint received to the final output power.

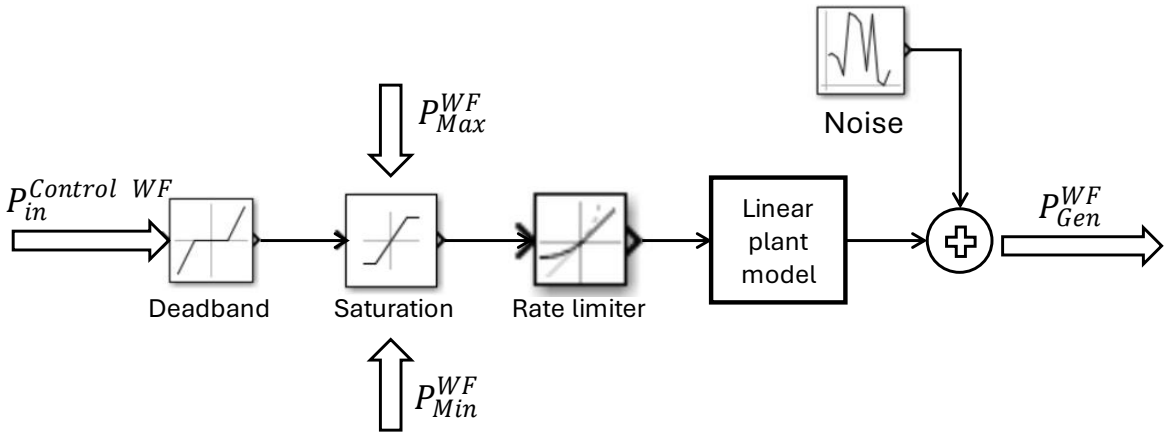

Figure 3. Schematic Operation of the Wind Farm Unit

The *Deadband* block simulates the deadband effect of each wind farm. This deadband represents a technical constraint: if the new setpoint power falls within a predefined tolerance range, it is considered insignificant, and the wind farm does not adjust its output to match the new setpoint.

This project simulates a non-ideal scenario in which the deadband configured in the BSP control algorithm is narrower than the actual deadband present in the wind farm model. This reflects cases where available data is inaccurate, representing a worst-case condition. Specifically, the BSP controller applies a deadband of ±1.5% of the wind farm's rated power, whereas the wind farm model applies a deadband of ±4.5%.

The subsequent block, *Saturation*, defines the upper and lower generation limits, ensuring the output remains within the permissible range between the estimated minimum and maximum available power.

To determine the minimum estimated power of the model, it is proposed to follow the cut-in wind speed. Reference [20] establishes that a cut-in speed of 3 m/s increases availability rates. Currently, most newly installed turbines have this cut-in speed. Globally, the most installed turbine brand is Vestas, as shown in [30]. Within this brand, the most commonly installed model is the V-100 [31], which also has a cut-in speed of 3 m/s [32].

The power generated at this speed varies by model, as the power curves differ. These curves represent the output power generated at different wind speeds. For the V-100 model, the power generated at 3 m/s is 49 kW (Figure 4 [33]), while its nominal power is 2000 kW [33], which corresponds to 2.45% of its nominal capacity.

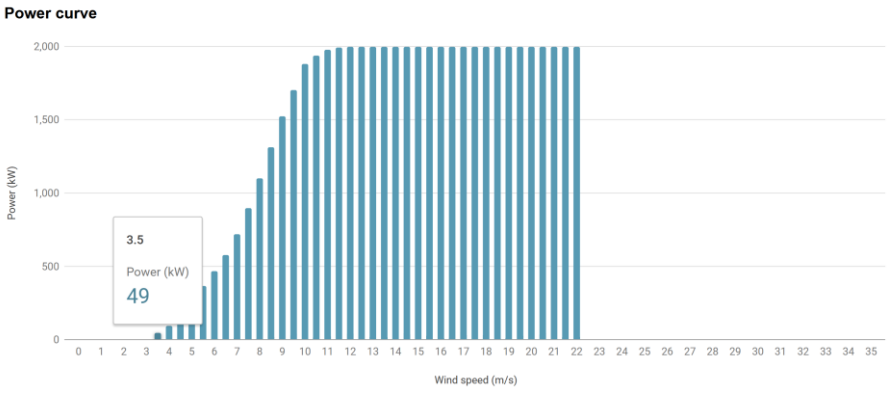

Figure 4. V-100 model power curve [33]

In this project, the wind farms considered are rated at 30 MW and 50 MW. Applying the same ratio (2.45%), the resulting output power at cut-in speed would be approximately 0.735 MW and 1.225 MW, respectively. Since this is the power produced when the turbines begin generating, it is reasonable to approximate these values to 1 MW and 2 MW, respectively.

Therefore, the estimated minimum power is set at 1 MW for 30 MW wind farms and 2 MW for 50 MW wind farms.

On the other hand, the maximum power is defined as the actual maximum output of the wind farms, which corresponds to the available wind power. However, unlike the wind farm model, the algorithms cannot directly access this real value and must rely on an estimation. The estimation is performed by dividing the real maximum power data into 15-minute intervals and calculating the average maximum power for each period. This approach is adopted because offering a maximum power close to the available wind power is economically advantageous, leading to higher profits.

The following blocks, *Rate Limiter* and *Linear Plant Model*, define the ramp rate limitation and the linear dynamic response of the generation system, respectively.

After these blocks, the output signal is processed through the *Noise* block, which introduces a 2 MW disturbance to simulate real-world measurement noise. In general, the results obtained with this block are not presented in this document so as to keep the figures clearer. However, they are specifically included in CHAPTER to demonstrate the correct operation of the algorithms under noisy conditions.

4.4 PERFORMANCE EVALUATION OF THE ALGORITHMS

The developed algorithms were evaluated using the System Operator's updated performance assessment framework. As previously explained, after secondary control operation, the

System Operator assesses the response to determine whether economic penalties should be applied in cases where the performance does not meet predefined operational standards.

The total power output generated by the BSP is compared against the setpoint power issued by the System Operator. Good performance is defined as accurately tracking the setpoint power without significant deviations.

Performance is classified into four categories, from best to worst:

- Active
- Error
- Alert
- Bad Response

The Bad Response category indicates large deviations sustained beyond an acceptable time threshold and is subject to penalties. Alert involves similar deviation magnitudes, but for shorter durations, remaining within the allowable time window.

Figure 5 illustrates how the performance evaluation is presented in this document. It is worth noting that at certain moments—such as at 10:00 a.m.—the graph may appear to show more than one evaluation result at the same instant (e.g., both Active and Error). However, this is not actually the case. The apparent overlap is due to the graphical representation: results are displayed as small squares within a limited space, which can cause visual overlap when evaluations change rapidly or occur in close succession.

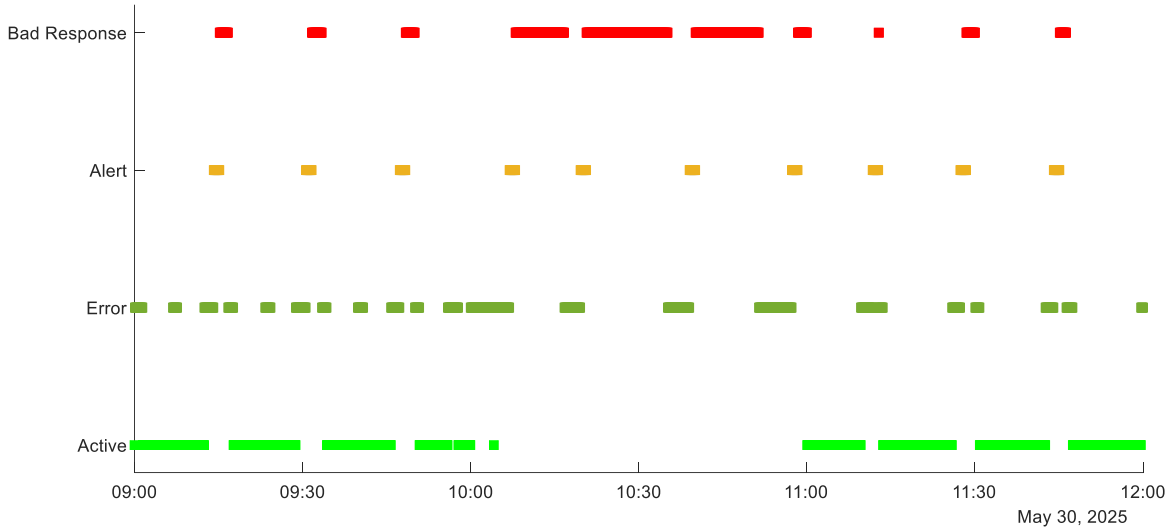

Figure 5. Example of How Performance Evaluation Is Presented

4.5 DIFFERENT TYPES OF ALGORITHMS

In this section, the algorithms developed in this project are presented, along with the main challenges and difficulties considered during their design, development, and implementation.

4.5.1 CHALLENGES THAT NEED TO BE ADDRESSED

To distribute the setpoint power provided by REE, it is essential to understand the various challenges the designed algorithms must address. First, they must comply with regulation requirements to balance the load and stabilise the system, regardless of the wind availability at any given moment. Wind energy is highly intermittent and unpredictable, unlike the conventional generation units described in [11]. Therefore, the algorithms must estimate the available wind power and distribute the setpoint accordingly among the wind farms. In contrast to [11], this project does not rely on conventional units to compensate for any shortfall in wind generation. Furthermore, to illustrate this main difficulty, Figure 6 is presented. This figure shows a 15-minute period, highlighting the available wind power,

represented as the real maximum power (P_{Real}^{WF} in Figure 6) alongside the estimated upper and lower power limits (P_{Max}^{WF} and P_{Min}^{WF}, respectively).

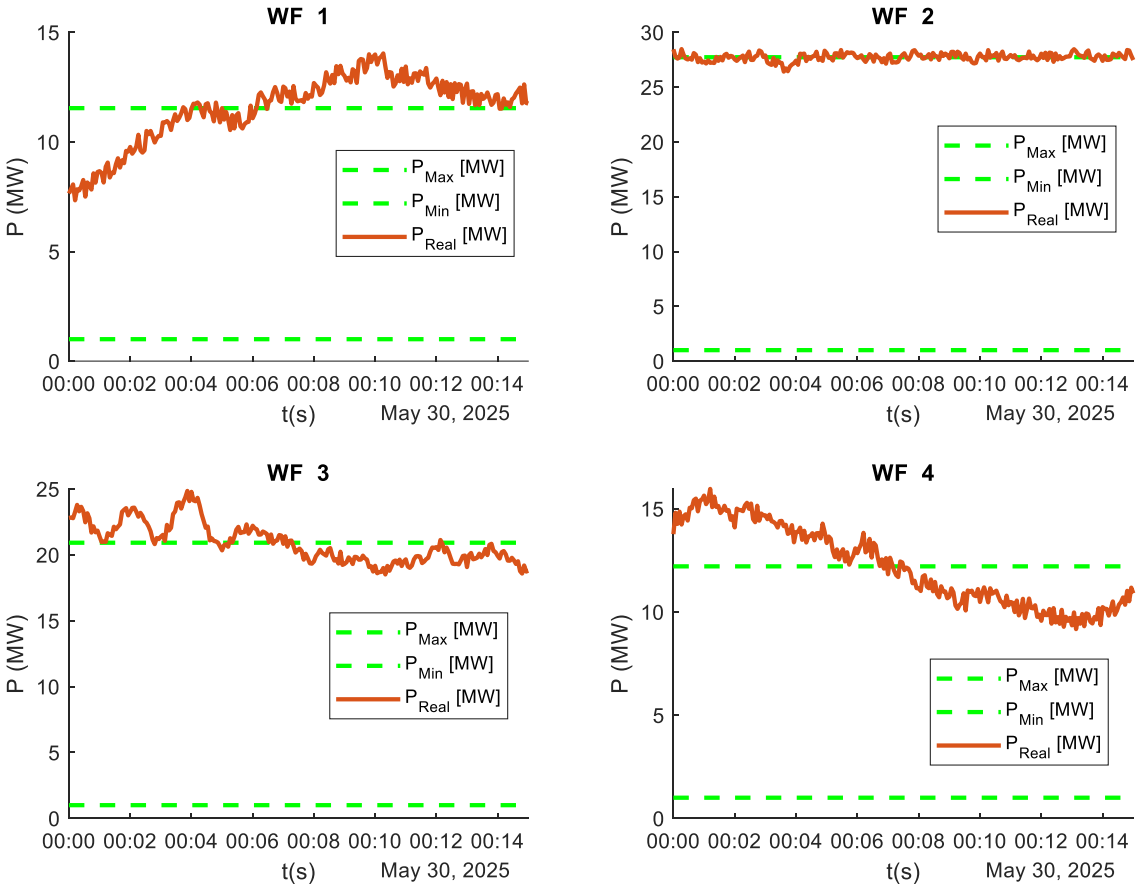

Figure 6. Graphical comparison of the real available maximum power and the estimated maximum power for the wind farms

In the case of the wind farm 2 (WF 2 in Figure 6), the estimation closely matches the real available power. However, for the other wind farms, the estimations deviate significantly from reality. For instance, if the algorithm is operating at time *t = 00:05*, it should ideally detect that the wind farm 1 (WF 1) is experiencing an increase in available power, though the estimation does not reflect this. In contrast, the wind farm 4 (WF 4) has more available power than estimated, but its wind availability is decreasing.

As a result, based on the estimation, the algorithm may allocate more power to the fourth wind farm rather than to the first, an appropriate decision according to the data it has, even if that data does not reflect the real situation. Additionally, in the wind farm 3 (WF 3), the available wind seems to be decreasing at $t = 00:05$, yet from that point onward, it increases. This highlights the inherent difficulty in accurately predicting wind availability, especially when recent outputs suggest the opposite.

Another difficulty is that the algorithms must operate across multiple wind farms over extended periods of time. As the number of wind farms and the simulation time increase, so does the complexity, since each farm has unique characteristics and behaviours that must be considered in the algorithm's design, challenges that may not arise when simulating shorter periods or with fewer units.

Moreover, the scenarios addressed in the literature differ from the one developed and analysed in this project. Most studies [15], [16], [17] involve battery storage systems or regulation zones that include both conventional and renewable energy sources. This makes it more difficult to identify previously tested technical solutions directly applicable to this case.

Additionally, some wind farms may not participate in regulation within the BSP. These farms will supply all the available energy without being controlled by the algorithm. This must be considered in the power distribution process.

Finally, the deadband, previously explained in section 4.3, presents an additional challenge. The algorithms must account for the fact that not all assigned setpoint power will result in actual generation due to deadband constraints. Furthermore, the deadband values known to the algorithm may be inaccurate and may not reflect the actual system behaviour. In the worst-case scenario, the real deadband could be significantly larger than assumed, affecting performance.

The following sections present the two developed algorithms.

4.5.2 MERIT ORDER ALGORITHM

This algorithm (Merit Order (MO)) distributes the system's input power based on the estimated maximum generation capacity of each wind farm. Initially, all wind farms are assigned a setpoint equal to their minimum power. This is because wind farms cannot ramp up or start quickly when required. Maintaining them at minimum output ensures they are ready to respond promptly when needed.

After this initial step, the units are ordered following a merit order list, and the algorithm begins with the first wind farm in the list and assigns to it a setpoint equal to its estimated maximum power. This process continues with more units following the list until the total desired power is assigned. The last wind farm in the sequence receives the necessary setpoint to complete the total desired power, which may result in this unit operating below its estimated maximum power. Non-regulating units, however, are always set to their maximum power.

See numbers 1 to 8 in Figure 7, which illustrate the entire allocation process described above.

This distribution method ensures that all available wind energy is utilised and not wasted. However, it leads to the saturation of most wind farms.

When distributing power, the algorithm also accounts for non-regulating wind farms. The estimated maximum power of these non-regulating units is subtracted from the total input power to be distributed, since they will independently generate all their available energy, closely aligned with the estimated values.

Additionally, the algorithm considers the power imbalance (error) from the previous simulation cycle, calculated as the difference between the previously distributed power and the actual power generated. It also includes the minimum power of wind farms whose estimated maximum and minimum power values are the same. These units have very low wind availability and then its output power cannot be controlled, helping to offset potential discrepancies between estimated and actual maximum power.

The adjustment of the input power is shown in the upper right corner of Figure 7.

Finally, the algorithm incorporates each wind farm's deadband. It checks whether the difference between the new setpoint and the previous cycle's setpoint exceeds the deadband threshold. If it does not, the setpoint is adjusted by adding or subtracting the deadband value plus 0.5 MW, depending on whether the regulation requires an increase or decrease in output. The additional 0.5 MW compensates for potential inaccuracies in the known deadband values.

Figure 7 illustrates the step-by-step process of the algorithm when the input power exceeds the generated power. It is important to note that all variables correspond to the executing cycle, except for the input power of each wind farm (used in the deadband check) and the control input power (used in the input power calculation for the executing cycle), both indicated with the superscript *PC*. In addition, the superscript *TWF* refers to the summation of the same variable across all wind farms in the BSP.

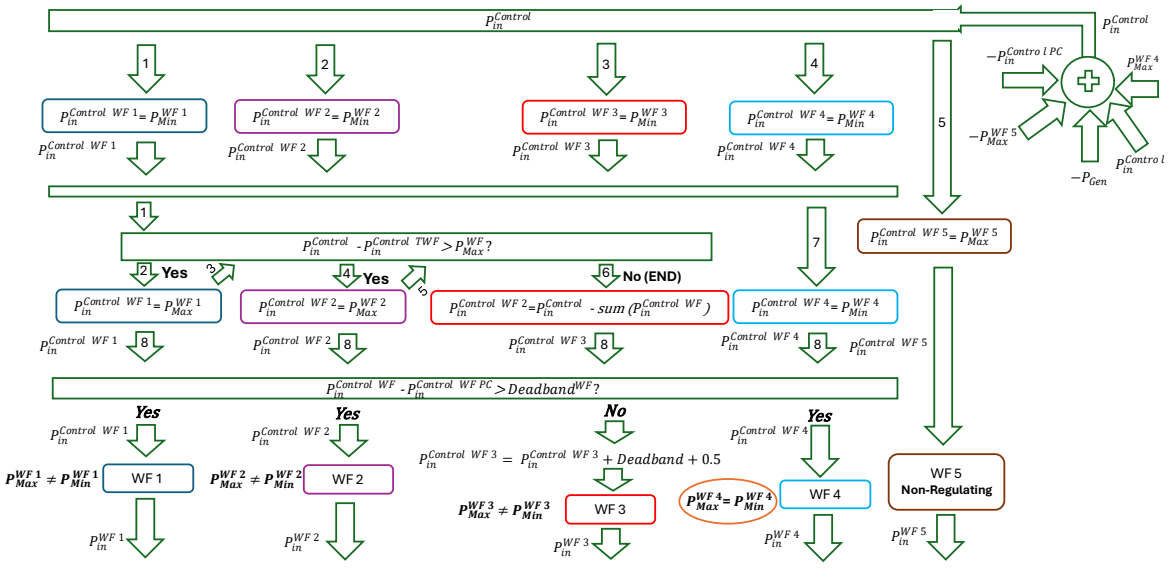

Figure 7. Diagram illustrating the process followed by the MO Algorithm

Figure 8 presents the output power of the six wind farms in a regulation zone. These particular wind farms were selected to facilitate a clearer explanation of the algorithm's performance. The units are ordered in the merit order list in increasing order of their wind farm number. In this figure (Figure 8), the generated power of each wind farm is shown in red, while each wind farm input power is represented in purple. the estimated minimum and maximum power limits of each wind farm are shown in green, and the actual maximum power (available wind) of each wind farm is displayed in yellow.

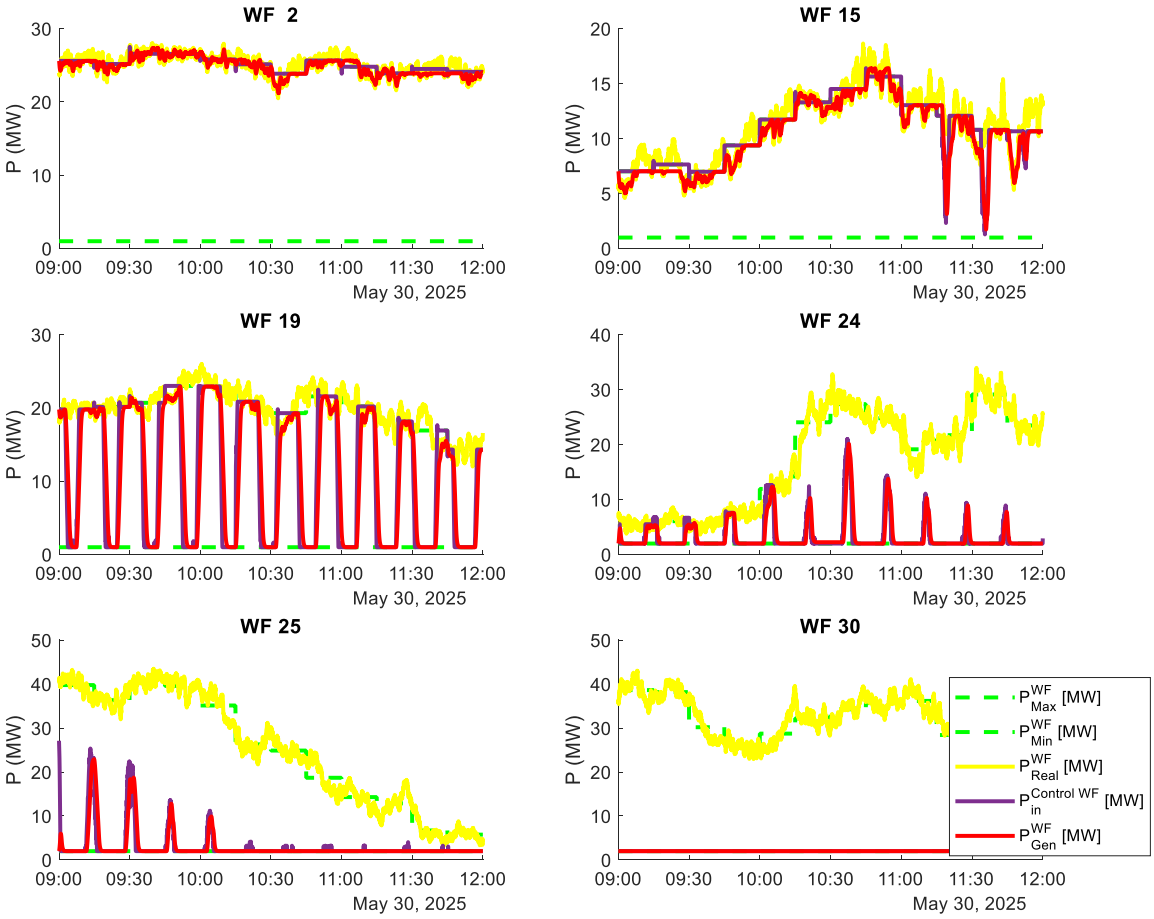

Figure 8. Operation of Six Wind Farms Using the MO Algorithm

It can be observed that Wind Farm (WF) 2 has a setpoint equal to its maximum estimated power; therefore, its output remains at that level. The output experiences fluctuations due to

changes in available wind power. As previously mentioned, the actual available power does not always match the estimation, which can constrain performance when it is lower than expected.

WF 15 behaves similarly to WF 2, except during the final hour of the simulation, when its output decreases nearly to the minimum estimated power because the total desired power is lower during that period.

WF 19 operates between its maximum and minimum estimated power values, providing regulation only during certain time intervals. Outside these periods, it remains at the minimum level, as defined by the algorithm.

WF 24 and WF 25 never reach their maximum output since they are rarely required to provide regulation. Consequently, they operate mostly at the minimum level.

It is noteworthy that WF 25 does not always follow its setpoint, specifically between 10:45 a.m. and 11:45 a.m. This deviation is due to the deadband: the algorithm operates with a smaller deadband than the real deadband of the unit (configured in the wind farm model). This does not represent the ideal scenario, as the intention was to simulate the worst-case conditions.

Finally, WF 30 remains at the minimum output throughout the entire simulation, as the required regulation power is fully supplied by the other wind farms listed above.

In conclusion, the simulation demonstrates three distinct behaviours:

- Some wind farms (e.g., WF 2 and WF 15) are saturated, constantly required for regulation.
- Others (e.g., WF 19, WF 24 and WF 25) actively regulate, with setpoints that vary based on system demands.
- The remaining units (e.g., WF 30) are inactive, operating at the minimum because total desired power is already fulfilled by earlier-listed wind farms.

Figure 9 presents the total desired power and the total power generated by the BSP for the case shown in Figure 8. As in Figure 8, the BSP's estimated maximum and minimum power are represented in green. In this figure, however, the total desired power is shown in red, while the total BSP generation is displayed in pink.

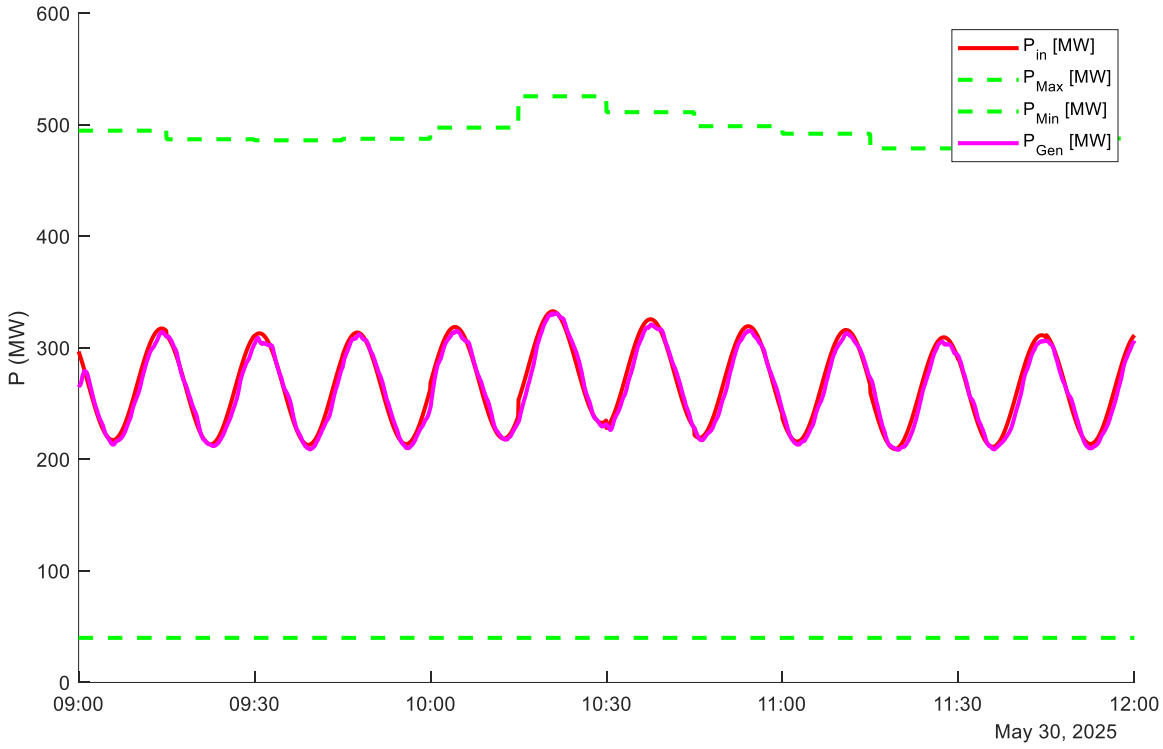

Figure 9. BSP Total Input and Output Power Using the MO Algorithm

4.5.3 PROPORTIONAL REGULATION BAND ALGORITHM

This algorithm (Proportional Regulation Band (PRB)) distributes the input power proportionally to the regulation band of each wind farm. The regulation band is defined as the difference between the estimated maximum and minimum power limits and the setpoint of the wind farm in the previous cycle.

Distributing power in this way prevents the wind farms from becoming saturated, enabling a faster response to sudden regulation demands. However, this method is highly sensitive to deadband constraints, since the proportional distribution often results in new setpoints that are very close to those of the previous cycle.

To mitigate this issue, the algorithm checks whether the deadband will affect each wind farm. If it does, the power that would not be supplied due to the deadband is redistributed using an alternative method. The affected wind farms are sorted by their available regulation band, and those with the largest bands are prioritised. These units receive a new setpoint equal to the previously distributed setpoint plus or minus 150% of the deadband (depending on whether the regulation requires an increase or decrease in power). If the remaining power is fully redistributed, the rest of the affected wind farms maintain the same setpoint as in the previous cycle.

As in the MO algorithm, the total desired power to be distributed is first adjusted by subtracting the estimated maximum power of the non-regulating units and by adding those with identical estimated maximum and minimum power. This is because they are expected to generate either a value very close to their estimated maximum or a certain power that cannot be controlled. This adjustment helps offset possible estimation errors. After this step, these wind farms are excluded from the rest of the distribution process, as they are considered to have no regulation band, as shown at the bottom of Figure 10.

However, unlike in the MO algorithm, the power imbalance (error) from the previous simulation cycle is not added to the distributed power in this case. Including it would lead to unstable setpoints for the wind farms, since the BSP is very sensitive with this algorithm: all WFs move simultaneously with small changes, and the output power from the previous cycle is highly variable. As a result, the calculated error constantly changes, affecting both the total input power and the input power assigned to each WF.

The detailed process explained above is illustrated in the diagram in Figure 10, where the total setpoint is higher than the generation at that moment. All variables correspond to the same executing cycle, except those with the superscript *PC*, which belong to the previous

cycle. It is important to note that variables with the superscript *TWF* refer to the summation of the same variable across all wind farms in the BSP. The variable *i* refers to the number of each WF.

Additionally, this diagram shows only two examples of units whose deadbands are not overcome, to simplify the figure. In reality, with more units whose deadbands are not overcome, the adjustment process is repeated. Each time a setpoint is increased by 150% of a unit's deadband, the total distributed power is checked. If the total desired power has been fully allocated, the algorithm finishes, and the remaining WFs retain their previous-cycle setpoints. If not, the next WF in ascending order of regulation band capacity has its setpoint increased by 150% of its deadband, and the total distributed power is checked again.

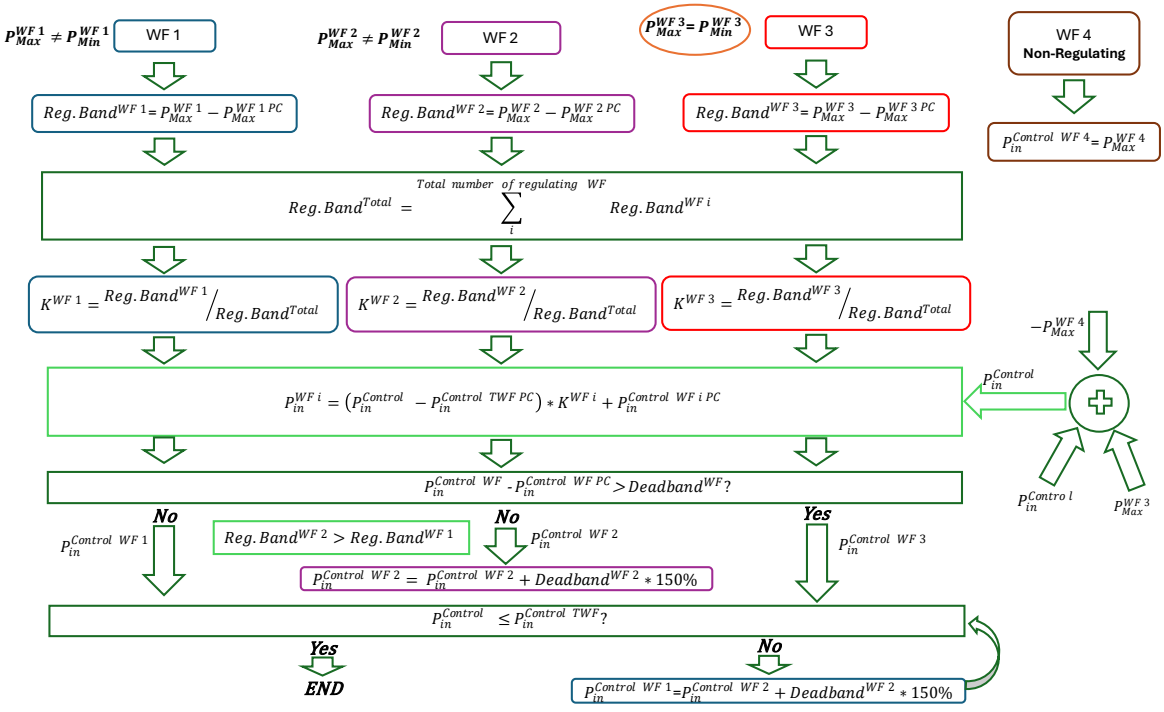

Figure 10. Diagram illustrating the process followed by the PRB Algorithm

The same simulation as in the merit order algorithm is performed now with the proportional algorithm, see input signal in Figure 11. The regulation zone has the same six units, and the

total desired power is the same as well. Figure 12 shows the operation of the six wind farms (WFs) to illustrate the performance of the algorithm. First, it is evident that all WFs operate around the middle of their regulation bands—none are saturated at either the maximum or minimum output. All WFs contribute to regulation at all times. This is the main objective of the algorithm and also its key distinction from the MO algorithm.

As shown in Figure 11, the BSP's generated power is less smooth than with the MO algorithm due to small jumps (±150% of the deadband) in each WF's setpoint as they attempt to overcome the deadband. This behaviour explains the minor fluctuations observed in the BSP's total generation.

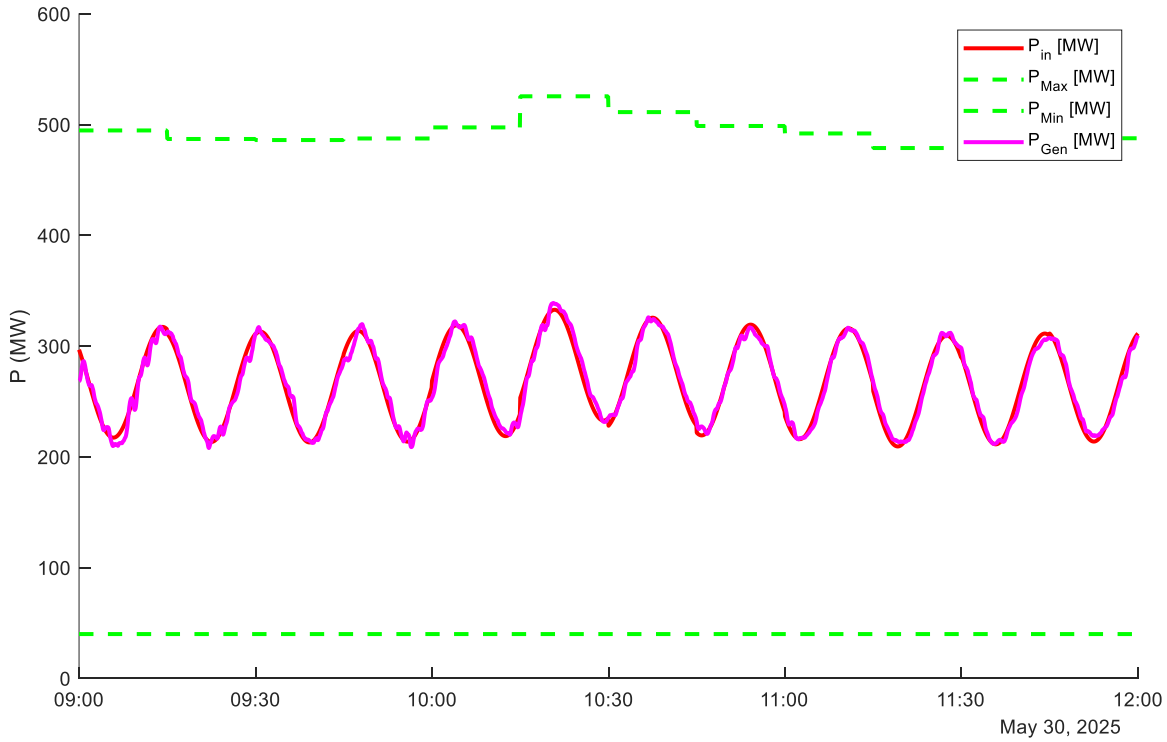

Figure 11. BSP Total Input and Output Power Using the PRB Algorithm

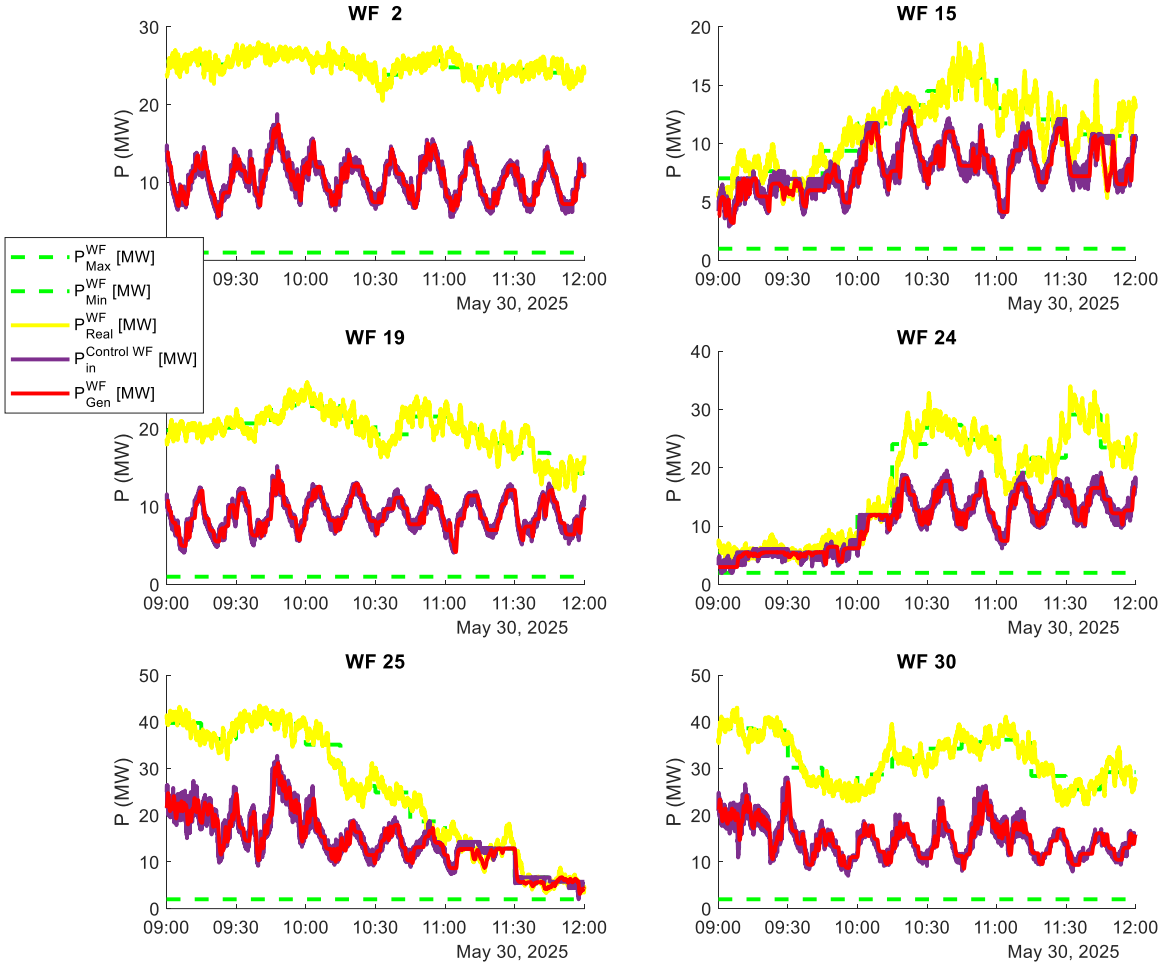

Figure 12. Operation of Six Wind Farms Using the Proportional Regulation Band Algorithm

Chapter 5. RESULTS AND DISCUSSION

The results of the regulation zone behaviour for different simulations using both algorithms are presented below. The simulated period spans three hours, from 9:00 a.m. to 12:00 p.m., including 30 wind farms in the regulation zone. Between 9:00 and 10:00 a.m., all units are regulating. From 10:00 to 11:00 a.m., the first five wind farms are non-regulating, while the others remain under control. Between 11:00 a.m. and 12:00 p.m., only the sixth wind farm becomes non-regulating, with all others continuing to operate under regulation. This is illustrated graphically in Figure 13.

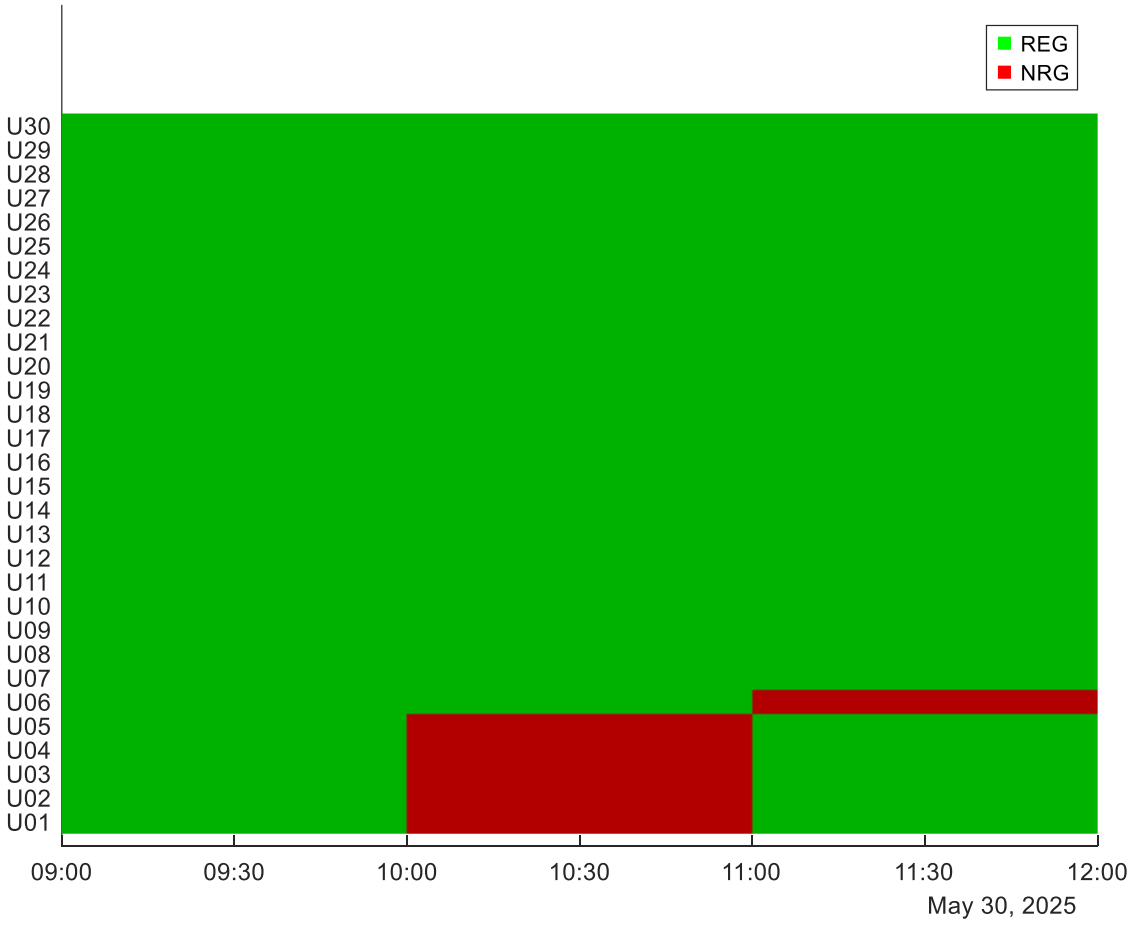

Figure 13. Regulating and non-regulating units throughout the simulated period

For each algorithm, four different input power signals from the System Operator (total desired power) are tested. The power scheduled in the day-ahead energy market is set at half the difference between the estimated maximum and minimum power, except for the third input signal, where a different value is used.

- **Sinusoidal signal**: Amplitude of 50 MW and a period of 1000 seconds (about 15 min).
- **Step signal:** An upward step of 80 MW at 10:30 a.m., followed by a downward step of the same magnitude one hour later.
- **Sinusoidal signal near the maximum power:** Amplitude of 100 MW and a period of 1000 seconds. In this case, the scheduled market power is set to 15 MW per wind farm, resulting in a total of 450 MW for the BSP. This signal poses a challenge to the algorithms, as the permissible upper regulation margins are reduced due to being calculated proportionally to the regulation band, which is significantly narrower in such scenarios.
- **Sinusoidal signal near the maximum and minimum power:** Amplitude of 224 MW and a period of 1000 seconds. In this case, both the upper and lower regulation margins are reduced.

5.1 MERIT ORDER ALGORITHM – RESULTS

Below are the results of applying the Merit Order Algorithm under different input signals.

5.1.1 RESULTS WITH SINUSOIDAL SIGNAL

In Figure 14, the total generation from all wind farms closely and acceptably follows the setpoint signal from the SO. This is further confirmed in Figure 15 , which presents the performance evaluation. Most of the time, the generation remains within the *Active* range, even during periods with a higher number of non-regulating units. Notably, between 10:30

a.m. and 11:00 a.m., there is no *Error* point, highlighting the algorithm's strong performance even under these conditions.

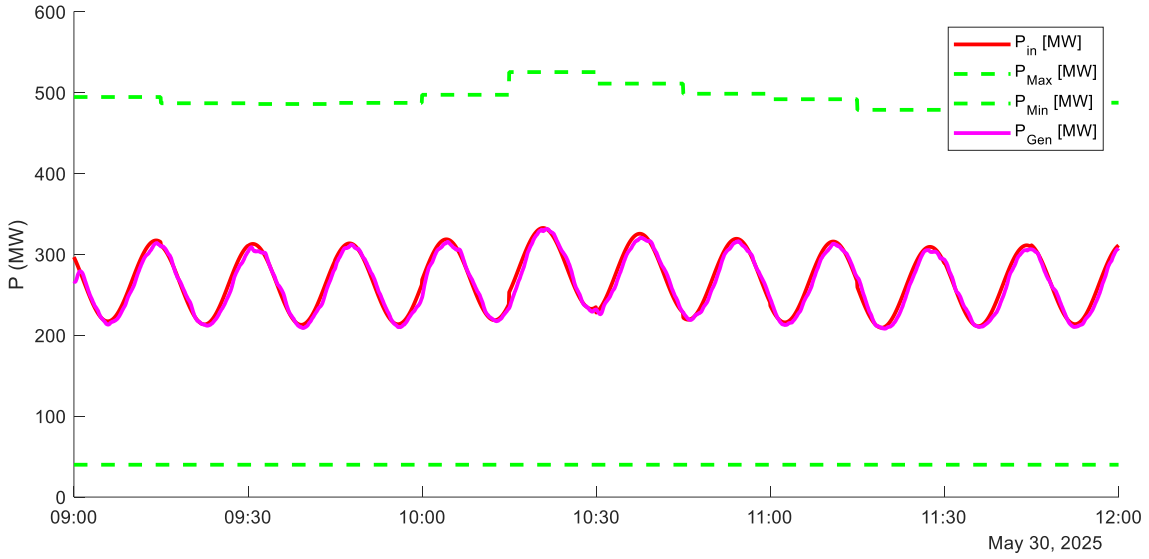

Figure 14. Results for the Sinusoidal Signal Using the MO Algorithm

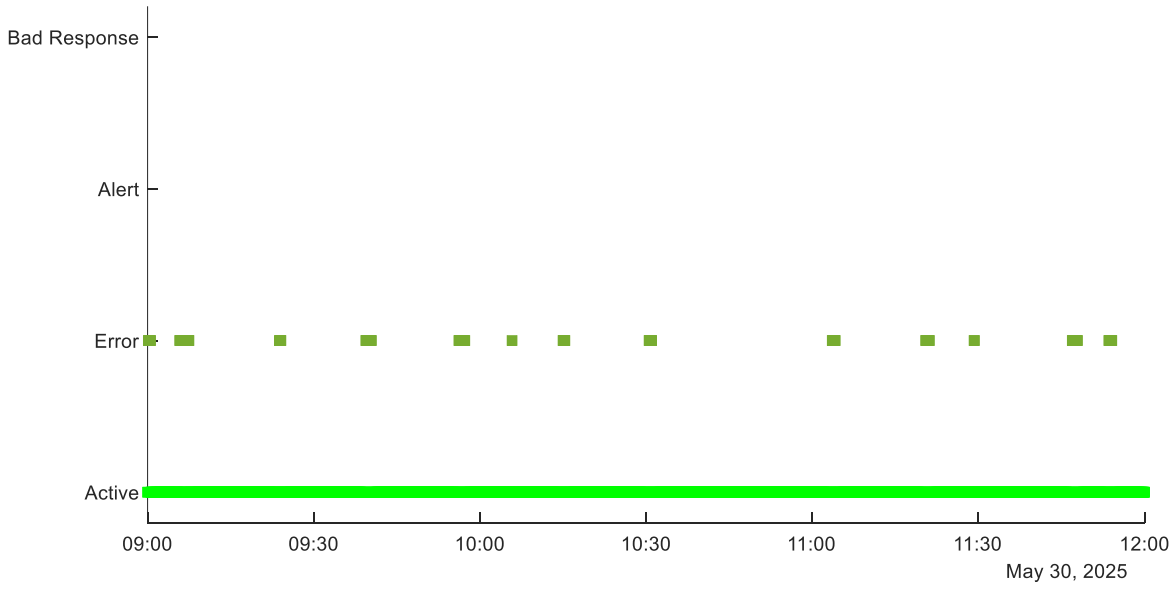

Figure 15. Performance Evaluation for the Sinusoidal Signal Using the MO Algorithm

As a result of using the MO Algorithm, most wind farms become saturated (i.e., they operate at their maximum limit). Only a subset of farms, specifically wind farms 15 to 25, as shown in Figure 16, are effectively regulating. Additionally, wind farms numbered 26 and above operate at their minimum output, since the system operator's setpoint is already fulfilled by the minimum output of all wind farms plus the remaining power distributed among the regulating units mentioned earlier. It is also noteworthy that WF 12 has identical maximum and minimum values, meaning it has no regulation band. This condition results from low wind availability, so its generation remains at the minimum most of the time.

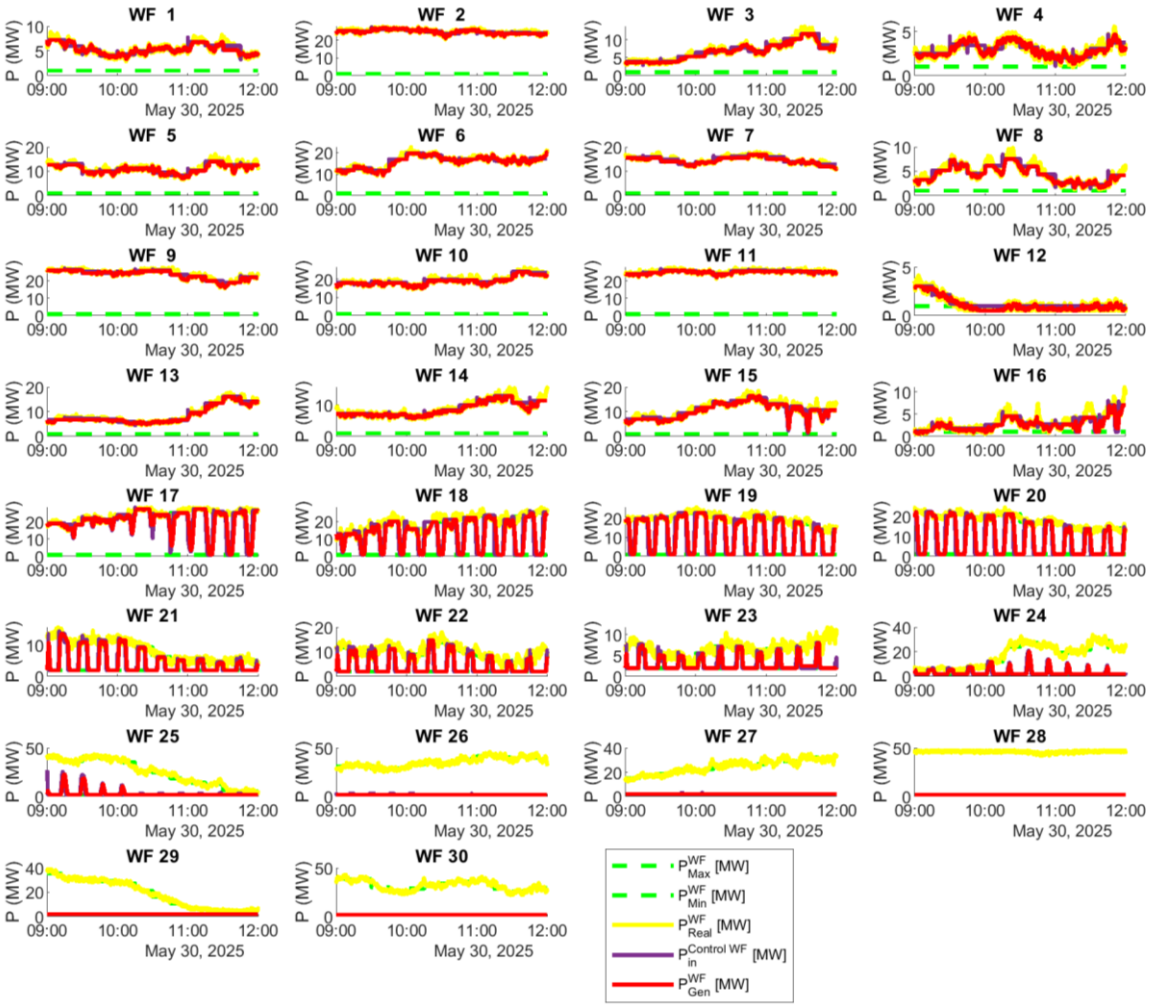

Figure 16. Individual Wind Farm Outputs for the Sinusoidal Signal Using the MO Algorithm

It is noticeable that most of the units are not affected by the deadband, as their generation always follows the setpoints. This confirms that the algorithm has successfully overcome that challenge.

5.1.2 RESULTS WITH STEP SIGNAL

Figure 17 shows the BSP performance. During both the upward and downward steps, the units respond quickly—an important aspect, as only a few units need to adjust their output in a very short period due to the nature of the algorithm. Moreover, their operation remains close to their setpoints. Some fluctuations are observed, as most units are operating at their maximum available power, which constantly varies due to wind conditions.

In Figure 17, some small steps can be observed throughout the entire simulation. These are caused by the 15-minute changes in the PTR signal. In this case, they are more noticeable compared to other simulations with different input power signals. The reason is that the step signal remains constant during the whole simulation (except at the step instants). For example, in Figure 14 they are barely noticeable. However, in this particular case, it can be clearly seen that the sinusoidal input power signal shifts its offset value due to the 15-minute changes in the PTR.

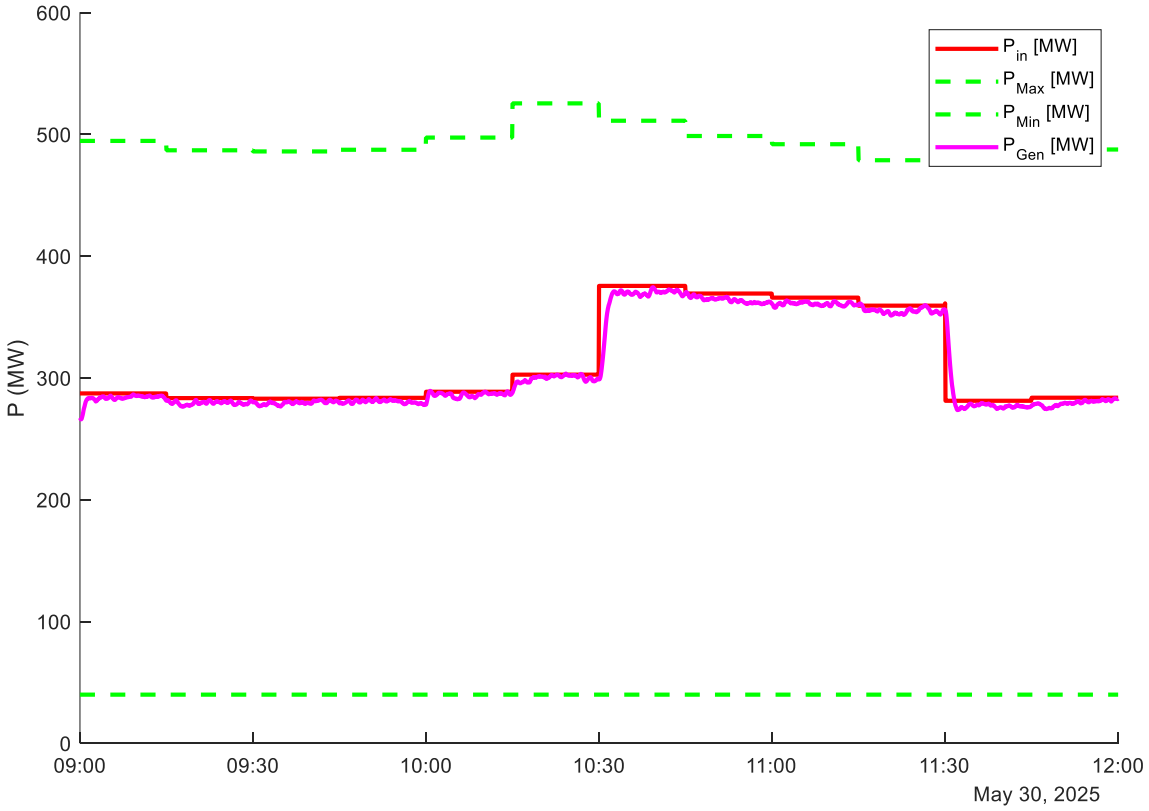

Figure 17. Results for the Step Signal Using the MO Algorithm

Interestingly, the step signal occurs halfway through the period with the highest number of non-regulating units, specifically between 10:30 a.m. and 11:00 a.m. The overall performance is slightly below the setpoint during this time, as the presence of more non-regulating units with higher setpoints introduces greater uncertainty. This effect is clearly demonstrated between 11:00 a.m. and 11:30 a.m., when only one non-regulating unit is active, and the generation more closely matches the setpoint.

Figure 18 presents the performance evaluation. It is important to clarify that although there appear to be periods where two evaluations occur simultaneously, this is not the case. This effect is simply due to space limitations in the representation and the need to display all data points.

It confirms the previous observations: the performance is highly accurate, as the BSP is not economically penalised during the simulation period. Notably, the response during the upward and downward steps is fast enough, as indicated by the *active* evaluation at 10:30 a.m. and 11:30 a.m.

Additionally, the highest concentration of error points occurs around 11:00 a.m., which aligns with the explanation provided in Figure 17. During this period, more units are in non-regulating mode, and the setpoint is higher. Moreover, the available wind at that time was lower than estimated for some units based on their maximum power, resulting in a total output below the expected level. A similar situation occurs around 11:50 a.m., again due to lower-than-estimated wind availability for certain units.

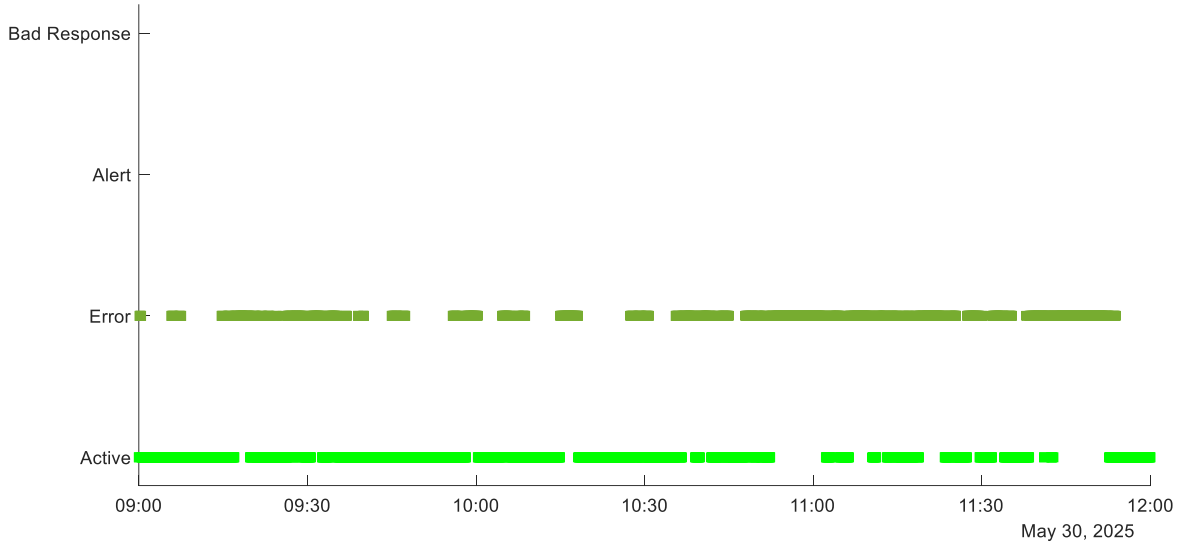

Figure 18. Performance Evaluation for the Step Signal Using the MO Algorithm

This case demonstrated that the algorithm enables a fast response to step signals. However, a drawback arises when following a constant setpoint, as the algorithm tends to saturate most units. This leads to a high dependence on the actual maximum power, i.e., the available wind, which is highly variable.

5.1.3 RESULTS WITH SINUSOIDAL SIGNAL NEAR THE MAXIMUM POWER

Figure 19 presents the overall performance of the BSP, with a zoomed-in view around the maximum, setpoint, and output power to facilitate understanding. In some periods, the setpoint exceeds the total available power in order to create a challenging scenario.

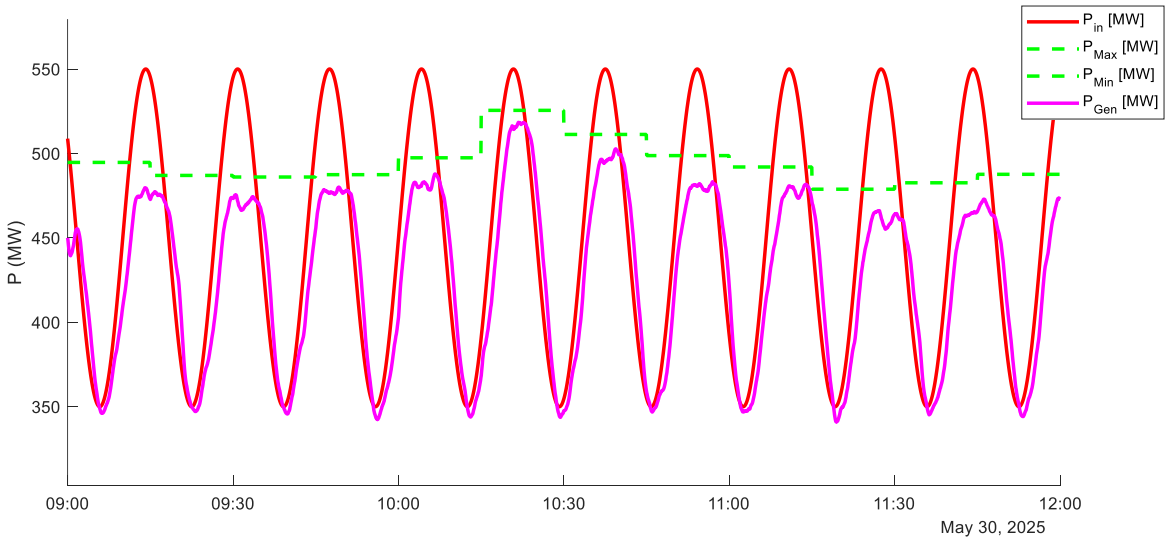

Figure 19. Results for the Sinusoidal Signal Near the Maximum Power Using the MO Algorithm (Zoomed View)

It is noteworthy that the BSP's response is slightly delayed compared to the setpoint. This delay is caused by rapid and substantial changes in the regulating setpoint over very short time intervals. In the case of the sinusoidal signal, this delay is not visible in Figure 14, unlike in Figure 19, because the vertical axis in Figure 19 is more zoomed in. Additionally, in this case, the required power increments are larger, demanding greater adjustments from the WFs.

When the setpoint exceeds the total available power, all units operate in active regulation. As a result, only a few wind farms must continuously alternate between their maximum and

minimum power over short periods. These few wind farms absorb the fluctuations, a task that would ideally be distributed among more units available in the BSP.

This suggests that, under this algorithm, the BSP does not have sufficient capacity to handle such dynamic changes, which leads to the observed delay.

Additionally, it is evident that the estimated maximum power is not entirely accurate. Even though all wind farms are operating at their maximum output, their total generation still does not match the estimated maximum power. Their actual performance remains below this value, indicating that the real maximum power imposes a constraint.

Figure 20 presents the performance evaluation. The BSP is economically penalised during the positive peaks of the sinusoidal signal, as the setpoint exceeds the maximum available power, making it impossible for the BSP to follow it. During these periods, the result is classified as *Bad Response*.

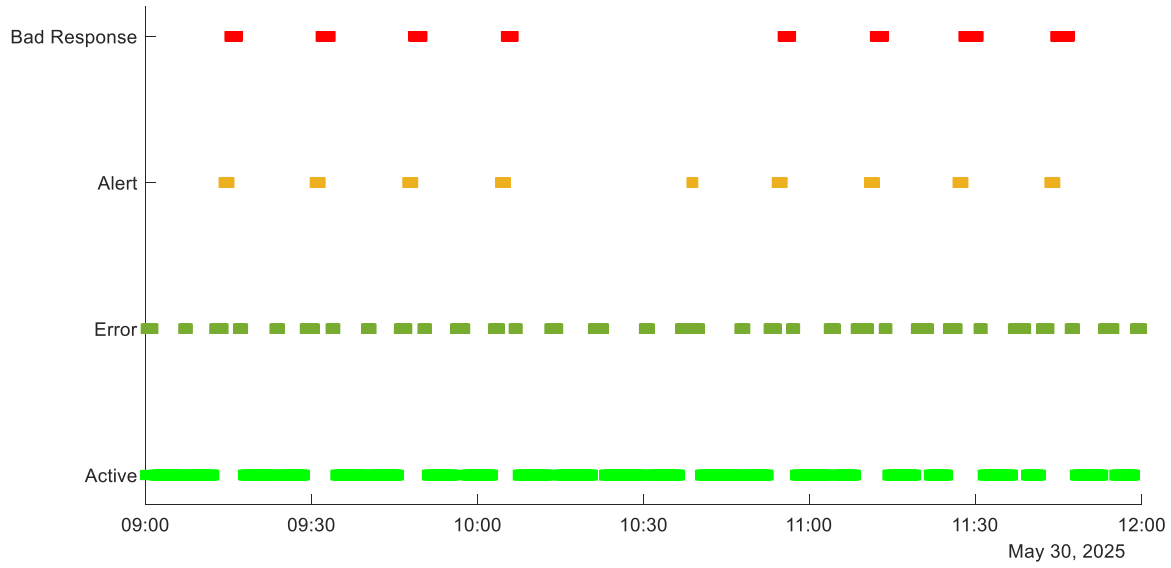

Figure 20. Performance Evaluation for the Sinusoidal Signal Near the Maximum Power Using the MO Algorithm

It can also be observed that *Alert* points appear just before the *Bad Response* points. These serve as early warnings, indicating that if the BSP's performance continues in the same manner, it will be classified as *Bad Response* and penalised accordingly.

For the remainder of the time, the BSP operates within the *Active* and *Error* evaluation zones. The *Error* points are primarily caused by the previously mentioned delay in the response.

5.1.4 RESULTS WITH SINUSOIDAL SIGNAL NEAR THE MAXIMUM AND MINIMUM POWER

The BSP performance under this signal is shown in Figure 21 , where a sinusoidal setpoint remains within the regulation band. Compared to Case 5.1.3 , the delay between the setpoint and the output is significantly reduced. This is because the setpoint moves continuously across the entire regulation band, requiring all units to adjust their output accordingly, as the full capacity of the BSP is needed.

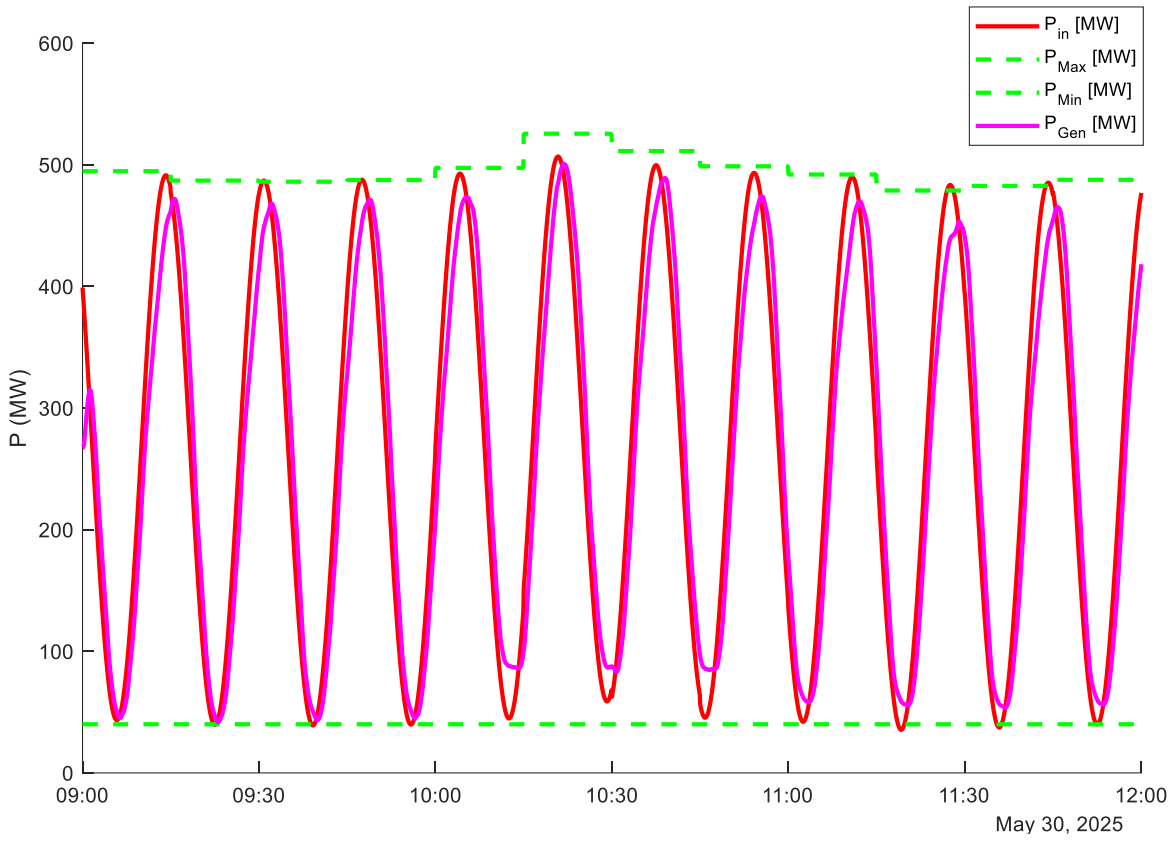

Figure 21. Results for the Sinusoidal Signal Near the Maximum and Minimum Power Using the MO Algorithm

Since all wind farms are simultaneously moving between their maximum and minimum power, the response is faster, and the delay is only noticeable during the positive peaks. During these peaks, the algorithm tends to push the units toward their estimated maximum power, which often exceeds the actual available wind. As a result, the units fail to reach the required peak output, and their generation falls short of the setpoint.

The algorithm does not detect this shortfall immediately, it only recognises it in the following cycle, when the previous setpoint is compared to the actual output. If a discrepancy is found, the algorithm compensates by adding this difference to the current setpoint in an attempt to follow the desired total output and estimate the current wind availability. This approach introduces a slight delay whenever the setpoint approaches the maximum available power.

Furthermore, during the periods with non-regulating units, between 10:00 a.m. and 12:00 p.m., the output does not reach the setpoint during the negative peaks. This occurs because all regulating wind farms are already moving across their regulation bands, and the BSP as a whole lacks sufficient capacity to follow the minimum setpoint. The non-regulating units remain constantly at their maximum power, leaving no available wind farms to provide the necessary downward regulation.

The operation of the entire BSP is very positive, as it remains within the *Active* evaluation zone most of the time, as shown in Figure 22. This confirms the good performance of the designed algorithm, especially considering that this represents the most challenging case for the BSP.

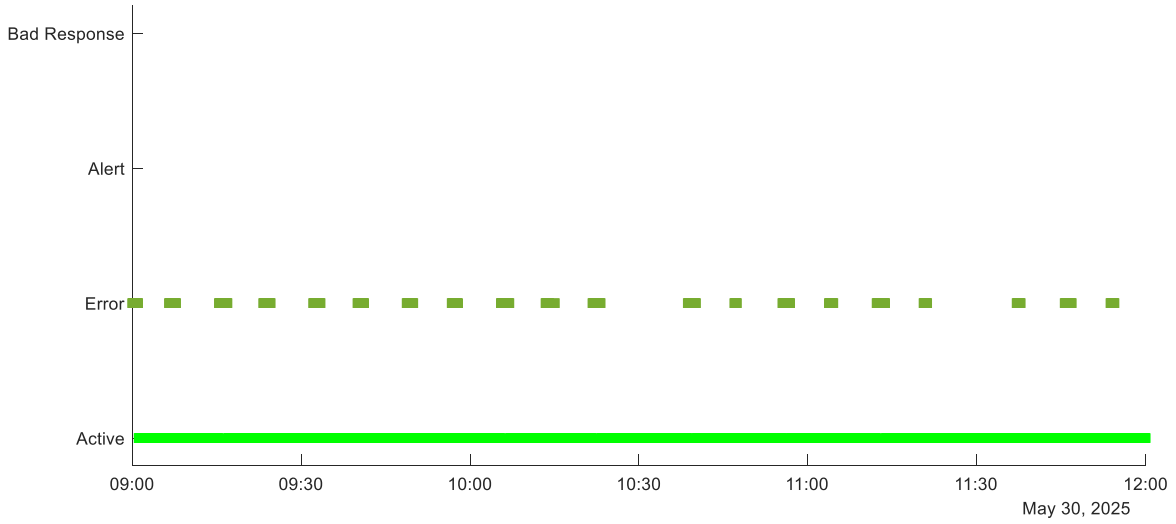

Figure 22. Performance Evaluation for the Sinusoidal Signal Near the Maximum and Minimum Power Using the MO Algorithm

5.2 PROPORTIONAL REGULATION BAND ALGORITHM – RESULTS

Below are the results of applying the Proportional Regulation Band (PRB) Algorithm under different input signals.

5.2.1 RESULTS WITH SINUSOIDAL SIGNAL

The BSP accurately follows the setpoint at all times, even when non-regulating units are present, as shown in Figure 23. Some steps can be observed in the output power; these occur because, in order to overcome the units' deadband, a value of ±150% of the deadband is added to the WFs affected by it.

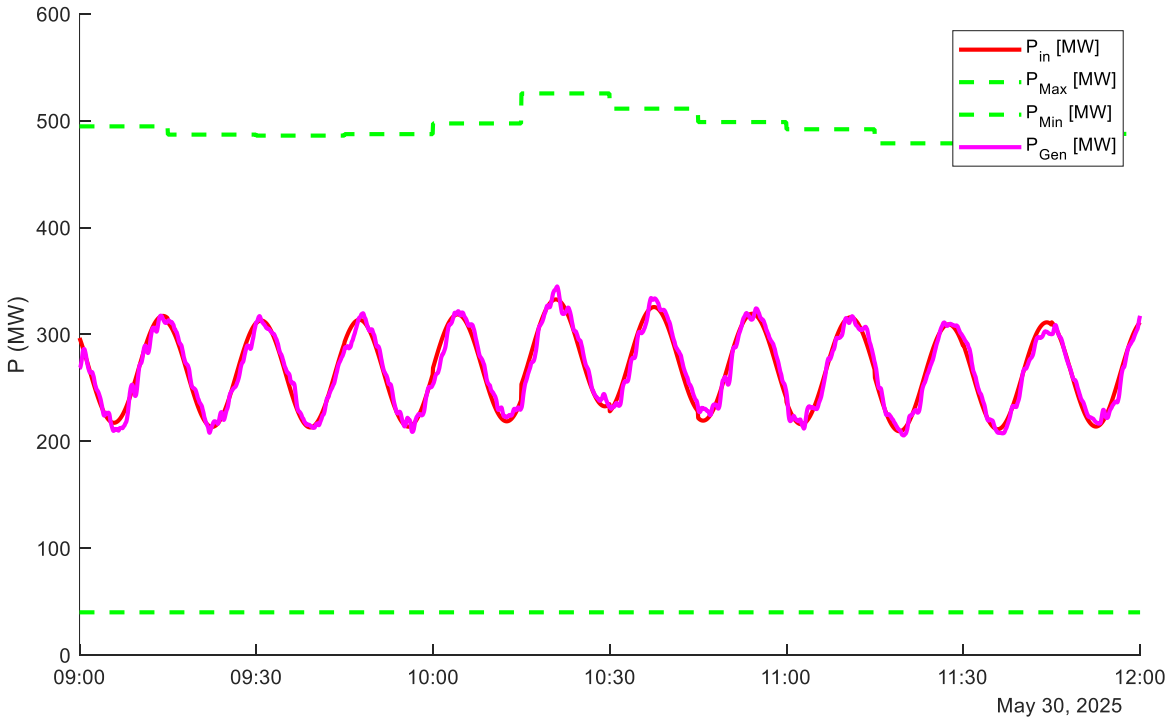

Figure 23. Results for the Sinusoidal Signal Using the PRB Algorithm

The good performance of the BSP with this setpoint signal using the proposed algorithm is confirmed in Figure 24, where the BSP remains mostly within the *Active* zone. Furthermore, the BSP is not penalised, as there are no *Bad Response* points. Notably, there are no *Alert* points either, although they do not incur a penalty, they represent the second-worst

evaluation outcome and serve as early warnings. Only a few points fall within the *Error* zone, caused by output steps that occasionally exceed the limits of the *Active* range.

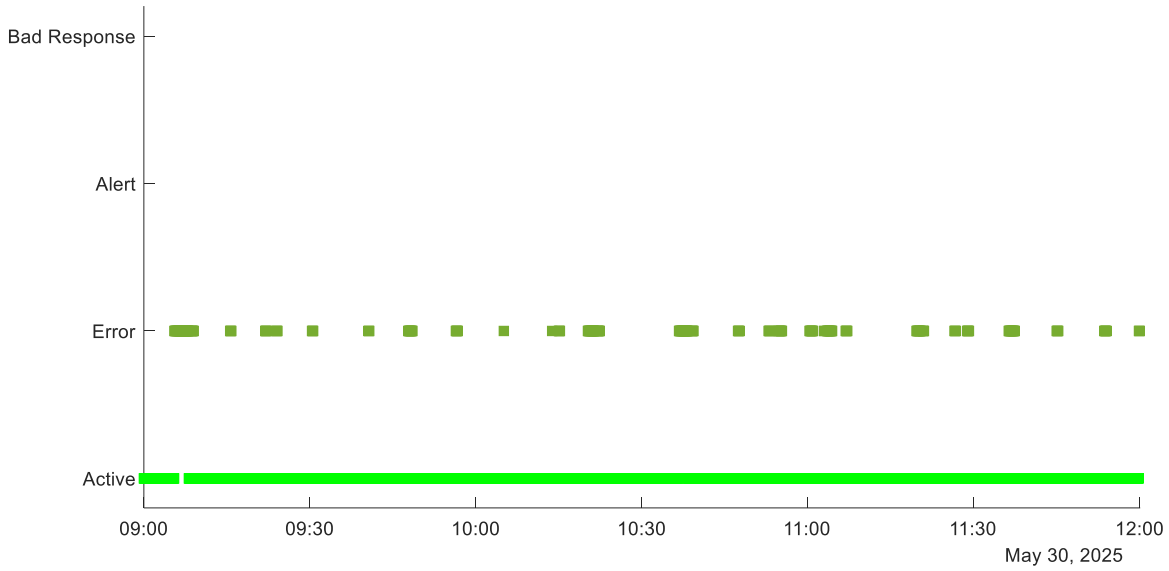

Figure 24. Performance Evaluation for the Sinusoidal Signal Using the PRB Algorithm

The performance of each unit is shown in Figure 25. As explained in Section 4.5.3., the units operate within half of their regulation band. The only saturated units are the non-regulating ones, which, by definition, operate using their entire available power—for example, WF 2 between 10:00 a.m. and 11:00 a.m. In this particular case, it is clearly visible that the WF switches between regulating and non-regulating modes, as its power jumps between the maximum and the setpoint, which is approximately at the midpoint of the regulation band. In contrast, in Figure 16, the WF is always at its maximum, making the mode change less apparent, since this WF is placed early in the list and the MO algorithm requires it to always generate at maximum power. As a result, managing such cases is more challenging for the PRB algorithm due to the large power jumps involved.

WF 12 is particularly noteworthy, as its maximum and minimum power are equal. This configuration is due to low wind conditions at its location, where the estimated maximum power falls below the defined minimum threshold. As a result, it has no regulation band and always operates at its maximum available power.

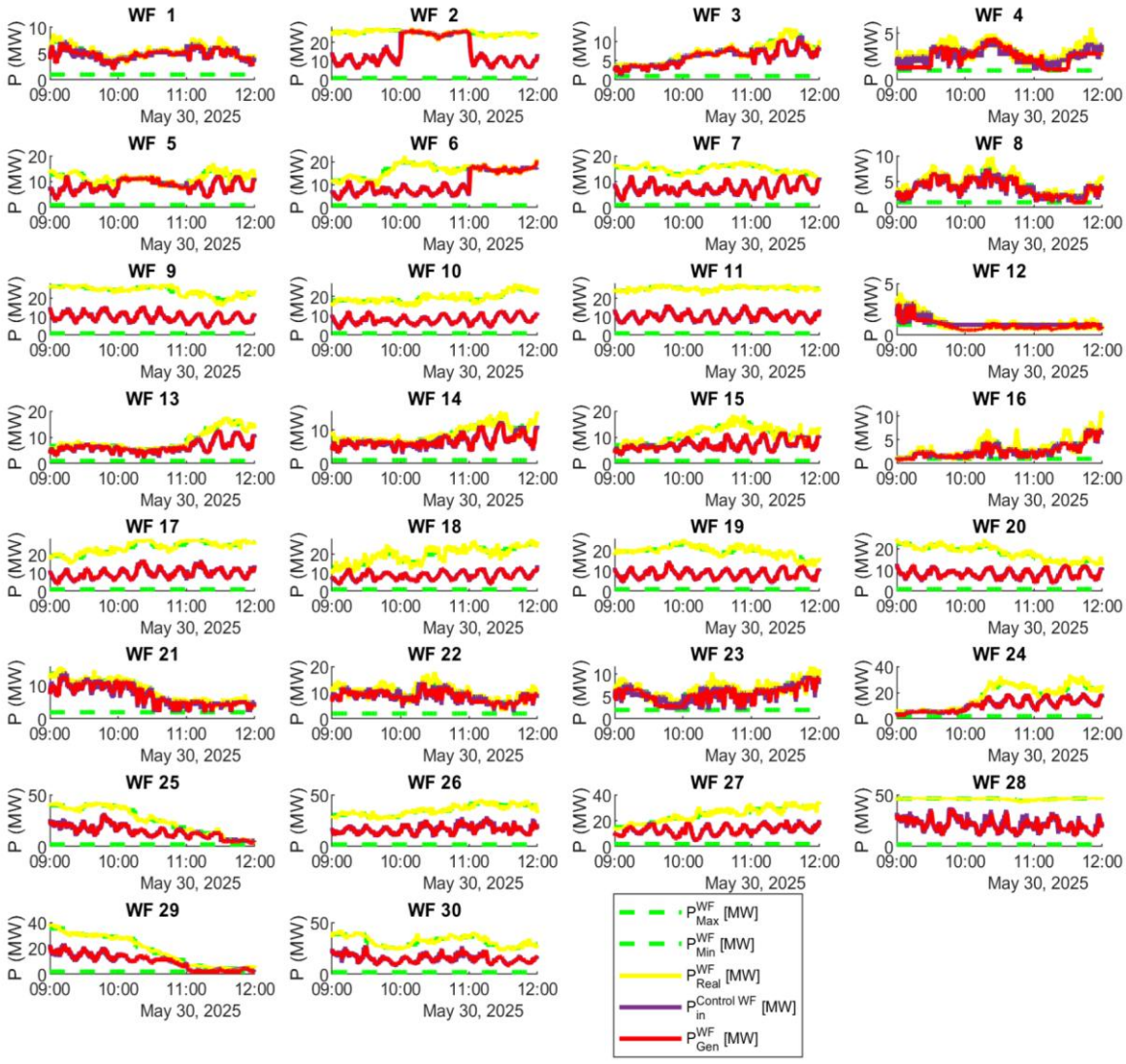

Figure 25. Individual Wind Farm Outputs for the Sinusoidal Signal Using the PRB Algorithm

Importantly, the algorithm successfully overcomes the deadband issue, as no wind farm is affected by it, as shown in Figure 25. This is a significant achievement, especially considering that, under this algorithm, distributing the setpoint proportionally results in very small increments and decrements, making units more susceptible to deadband effects than with the MO algorithm.

5.2.2 RESULTS WITH STEP SIGNAL

Figure 26 presents the BSP performance under the utilization of the PRB algorithm. At all times, the total operation of the units closely follows the total input power, even when non-regulating units are involved. The operation fluctuates slightly around the input power due to the nature of the algorithm. As previously explained, the algorithm attempts to overcome the units' deadband by setting a setpoint that increases each deadband by 150%. Compared to the MO algorithm, the PRB produces more fluctuations; however, it tracks the setpoint more accurately. For instance, while in Figure 17 the generation remains consistently slightly below the setpoint, in this case the response is noticeably closer. Ultimately, the choice of the preferred algorithm depends on whether smoother generation (as in the MO) or more accurate setpoint tracking (as in the PRB) is prioritised.

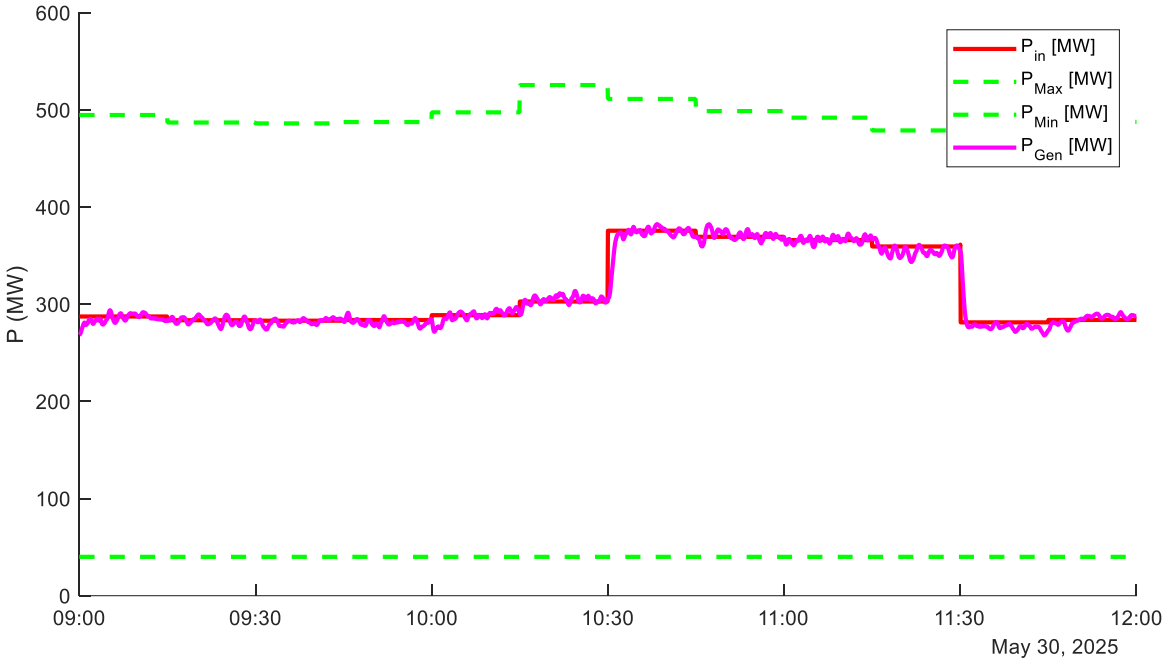

Figure 26. Results for the Step Signal Using the PRB Algorithm

Furthermore, the changes in total operation occur very rapidly, as all the WFs respond simultaneously, without significant increases or decreases in individual operations. Notably, the downward step is executed faster than the upward step.

The evaluation of this simulation is shown in Figure 27, where the BSP operates within the *Active* and *Error* zones. This confirms the good performance of the algorithm with step signals and constant values: as explained, the operation consistently follows the input signal with high accuracy. The *Error* points are due to small fluctuations that exceed the boundaries of the *Active* zone.

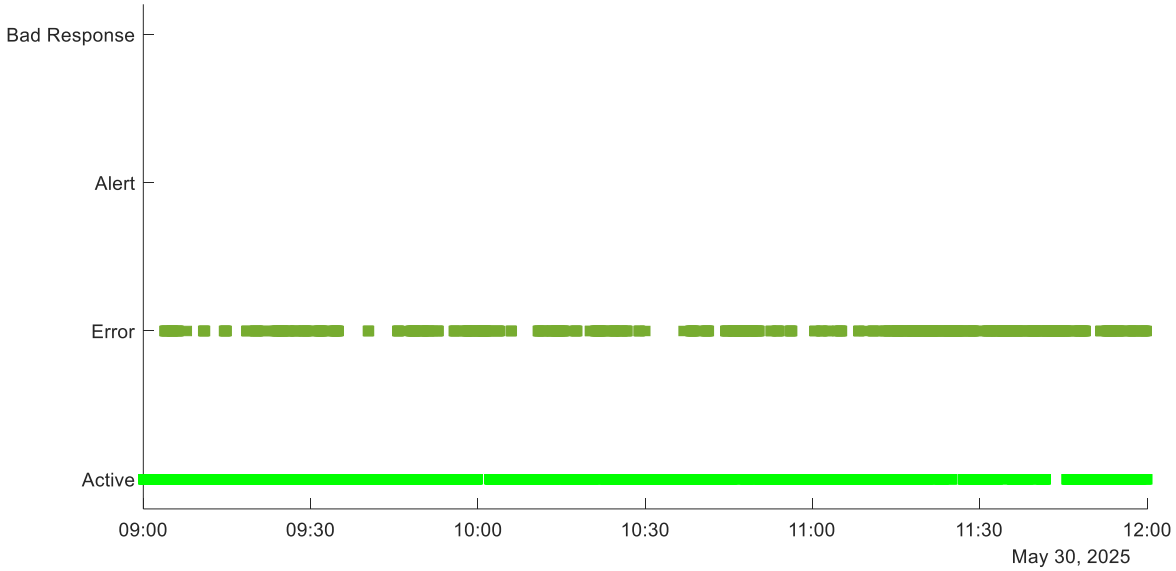

Figure 27. Performance Evaluation for the Step Signal Using the PRB Algorithm

5.2.3 RESULTS WITH SINUSOIDAL SIGNAL NEAR THE MAXIMUM POWER

Figure 28 shows a zoomed-in view of the total output power, input signal, and maximum power. The performance of the BSP with the Sinusoidal Signal Near the Maximum Power is highly accurate, as the generation follows the input signal at all times without noticeable difference or delay. This is achieved because all units move simultaneously, and each adjusts its output proportionally to its regulation band, resulting in small, smooth changes.

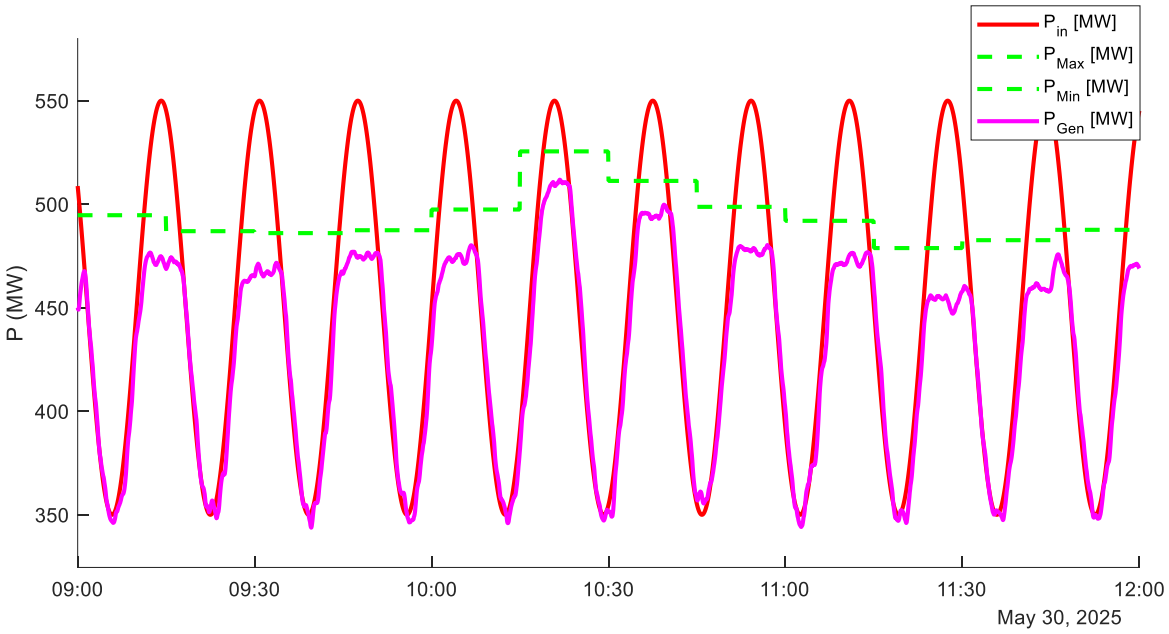

Figure 28. Results for the Sinusoidal Signal Near the Maximum Power Using the PRB Algorithm (Zoomed View)

It is worth noting once again that the estimated maximum power does not match the actual available power. At the positive peaks, where the setpoint exceeds the estimated maximum power, generation is constrained by the real wind conditions, which are lower than expected.

Figure 29 presents the evaluation of the BSP's operation under this algorithm and input signal. The BSP is economically penalised (*Bad Response* points) during the positive peaks of the sinusoidal input signal, as expected, since the setpoint exceeds the maximum available power. *Alert* points also appear, serving as warnings preceding *Bad Response* evaluations.

Even so, the BSP still achieves a greater number of *Active* points than *Error* points, indicating generally good performance.

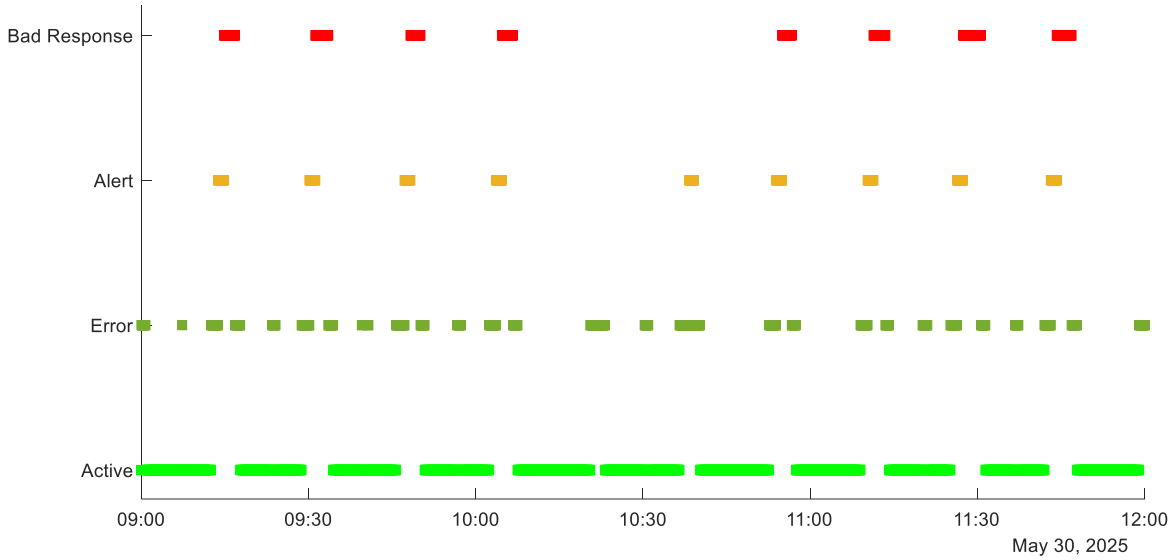

Figure 29. Performance Evaluation for the Sinusoidal Signal Near the Maximum Power Using the PRB Algorithm

5.2.4 RESULTS WITH SINUSOIDAL SIGNAL NEAR THE MAXIMUM AND MINIMUM POWER

Figure 30 shows the good performance of the PRB algorithm with this input signal. The generation closely follows the setpoint power at all times, except during the signal peaks. At those moments, the output is constrained by the actual maximum power, similarly to what was observed in Section 5.2.3, and by the deadband during the negative peaks. While the deadband constraint is mostly overcome, some units operate very close to their minimum power when attempting to reach the lowest points of the input signal, and the remaining margin falls within the deadband. In such cases, the algorithm cannot further reduce the input to overcome the deadband, as this would require setting a power level below the technical minimum, risking the shutdown of the wind farms.

Additionally, during periods when non-regulating units are present in the BSP, it becomes more difficult to reach the negative peaks of the setpoint power. These units always operate

at their maximum available power and cannot reduce output, thus limiting the BSP's ability to lower the total generation.

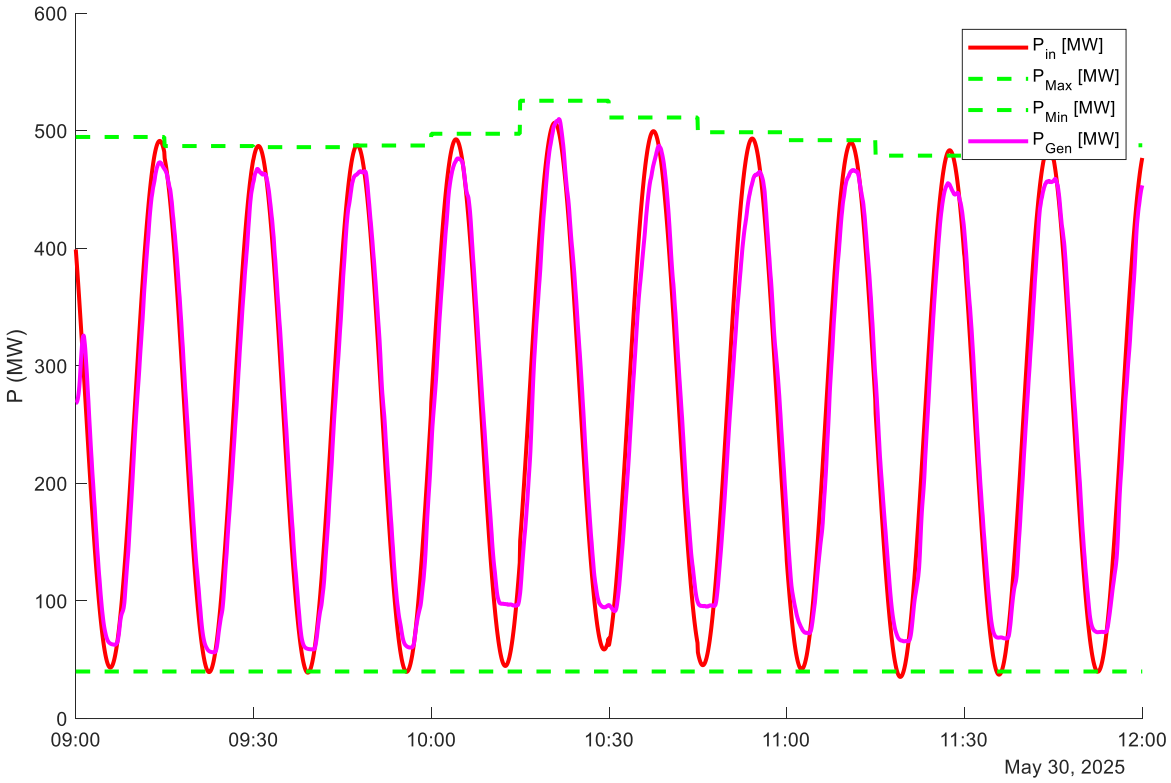

Figure 30. Results for the Sinusoidal Signal Near the Maximum and Minimum Power Using the PRB Algorithm

A particularly notable moment is the positive peak around 10:20 a.m., where the generation successfully matches the setpoint. This is the only positive peak reached, thanks to a higher estimated maximum power in that 15-minute interval, which indicates more wind availability and therefore no limitation on the generation. In contrast, with the MO algorithm this situation does not occur, as the large changes in generation introduce a delay. Although the setpoint of each wind farm is set to its maximum, there is not enough time for the

generation to fully reach the setpoint at the peak, and the total generation consistently remains below it.

Figure 31 presents the evaluation of the most challenging simulation for this algorithm, as the setpoint power spans the entire regulation band. Despite this, the evaluation remains highly favourable: there are only a few *Error* points, while the rest fall within the *Active* zone.

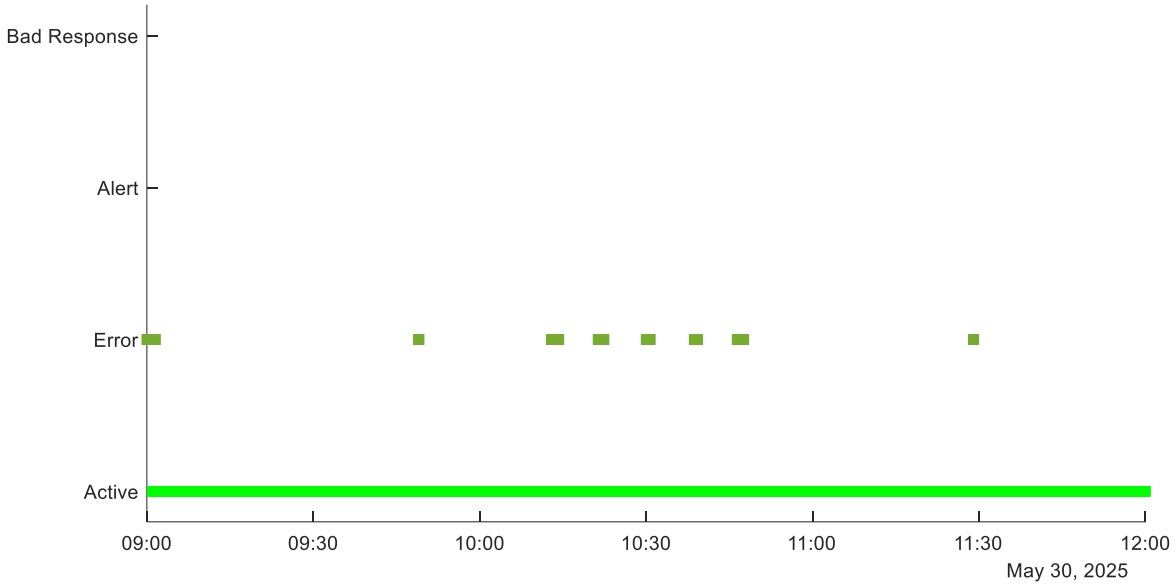

Figure 31. Performance Evaluation for the Sinusoidal Signal Near the Maximum and Minimum Power Using the PRB Algorithm

Most of the *Error* points occur when the BSP is unable to reach the minimum peaks of the input signal, particularly during periods with a higher number of non-regulating units. This simulation stands out as the best, with the highest number of *Active* points, confirming the strong performance of the algorithm. The evaluation with this algorithm is better than with the step signal or the sinusoidal signal because it handles larger power increments and rapid changes more effectively. All units move simultaneously, and the algorithm is very sensitive to small changes due to the deadband, as explained previously.

5.3 SIMULATIONS WITH NOISE – RESULTS

In this section, the developed algorithms are tested using a random noise with an amplitude of 2 MW in the wind farm generation signal to emulate real-world measurement noise. The input signal to the BSP is a sinusoidal waveform oscillating near the system's maximum and minimum power—the same used in the previous simulations—as it represents the most challenging case.

5.3.1 MERIT ORDER ALGORITHM

Noise is simulated with this algorithm. As shown in Figure 32, generation closely follows the input power. The evaluation of this simulation is presented in Figure 33, where the results are classified as *Active, Error*, and *Alert*. Most of the time the evaluation falls within the first two categories, although points within the *Alert* classification are observed throughout the entire simulation period. This confirms that the algorithm operates similarly to the case without noise, with slightly degraded performance as expected due to the noise.

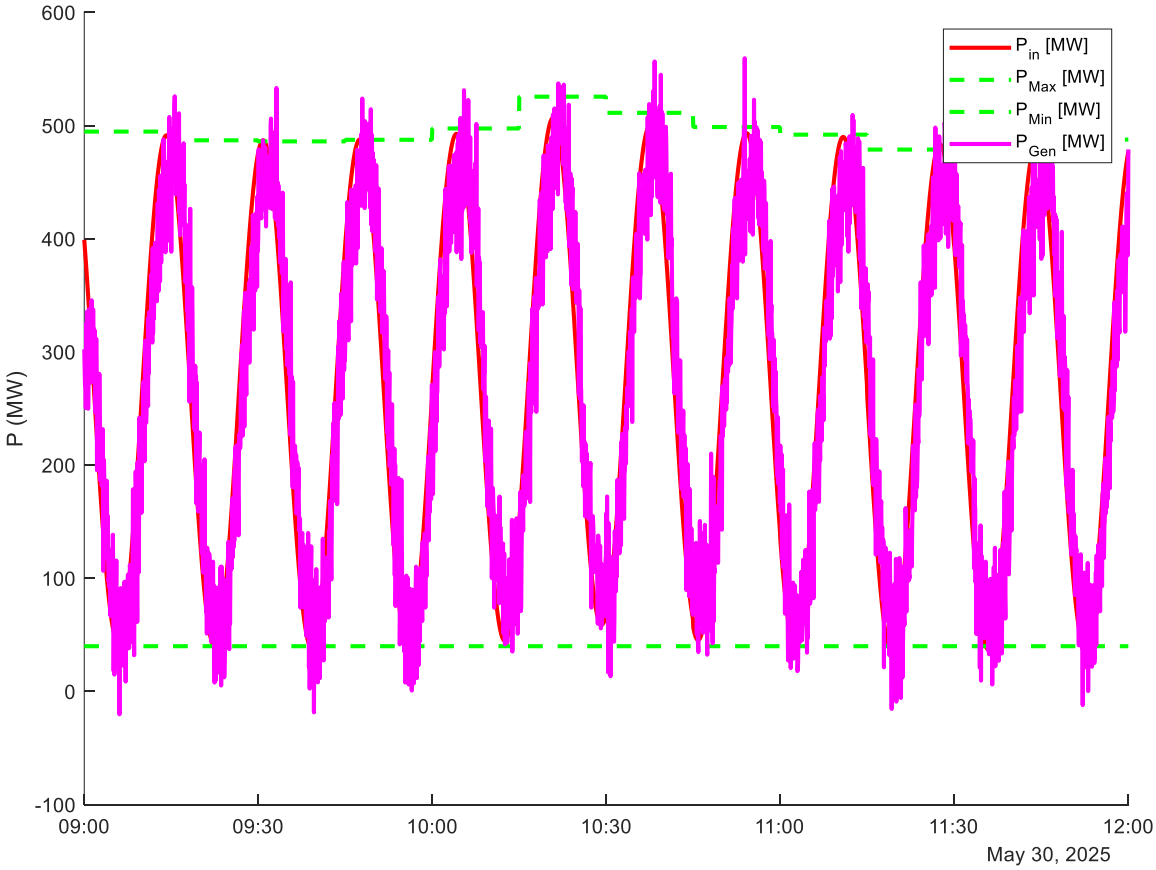

Figure 32. Results of the MO Algorithm with Noise

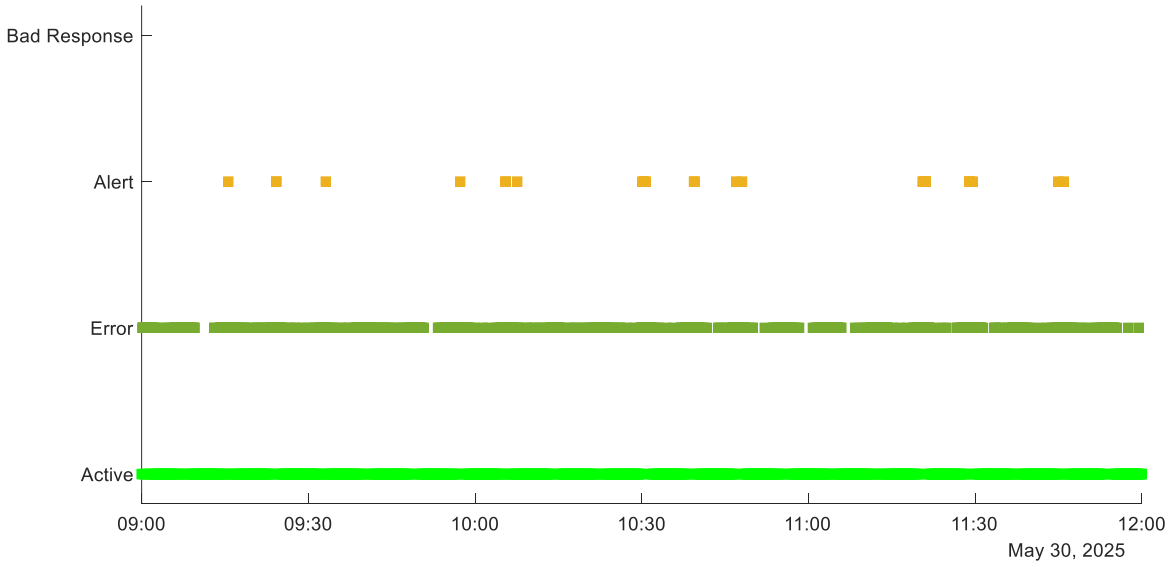

Figure 33. Performance Evaluation of the MO Algorithm with Noise

5.3.2 PROPORTIONAL REGULATION BAND ALGORITHM

Again the model is simulated with the input signal and measurement noise, but with the PRB algorithm. Despite the noise, the output power closely follows the input signal, as shown in Figure 34. This is further confirmed in Figure 35, where the evaluation is classified mostly as *Active* and *Error*. The remaining parts of the simulation are labelled as *Alert*, occurring during periods when non-regulating units are present. Only a few instances of *Alert* are observed. As explained in Section 5.3.1, the algorithm's performance with noise remains robust, with only slight degradation as expected. This confirms its reliable operation, even under realistic conditions where signals are affected by noise.

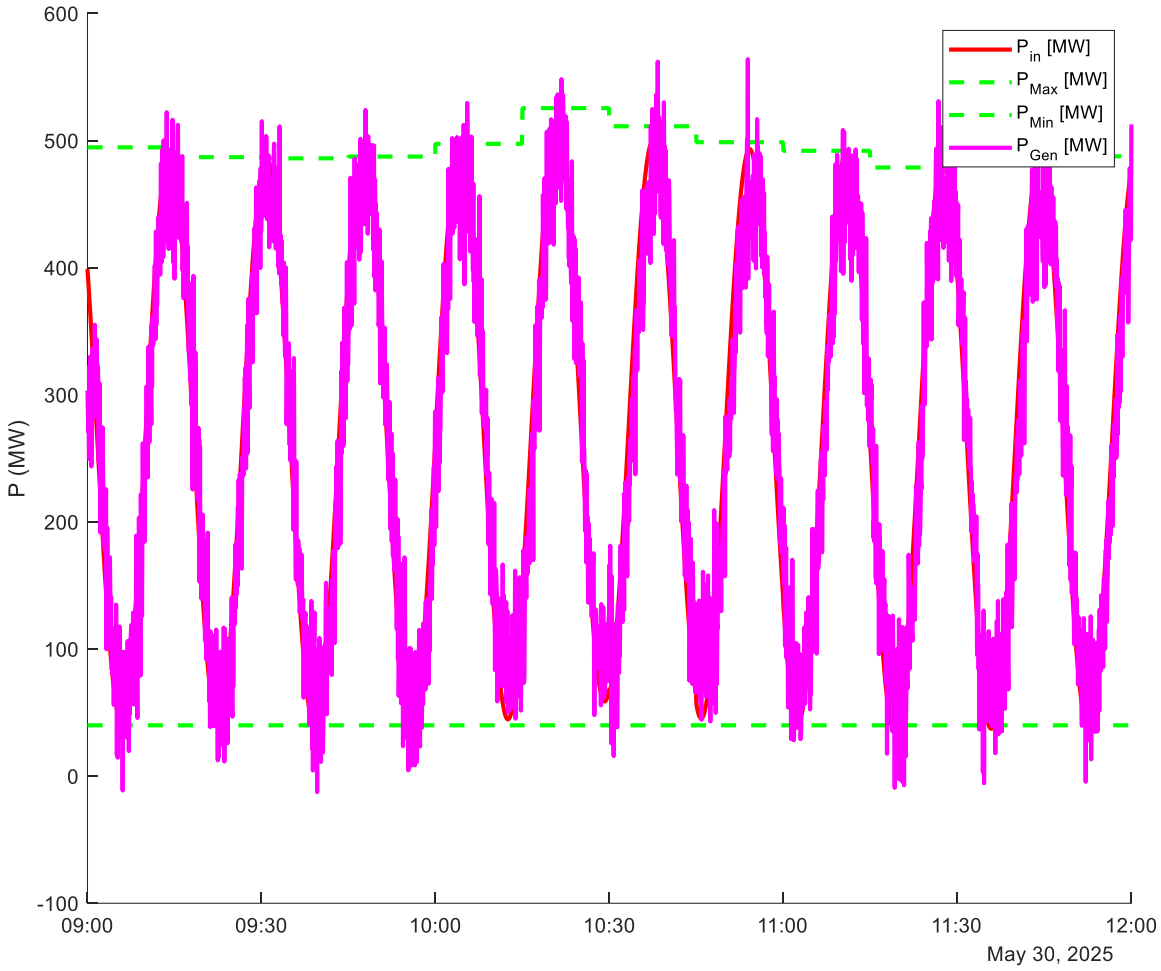

Figure 34. Results of the PRB Algorithm with Noise

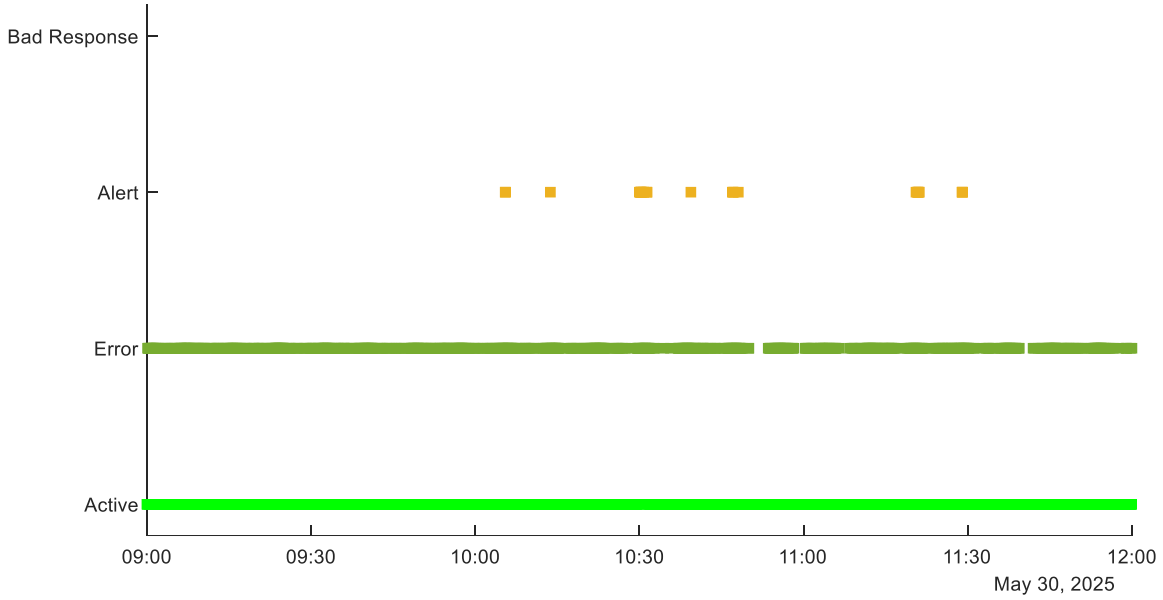

Figure 35. Performance Evaluation of the PRB Algorithm with Noise

Chapter 6. CONCLUSIONS AND FUTURE WORK

In this project, two different AGC algorithms for a regulation zone were developed to meet the necessary requirements for integrating renewable technologies into the secondary frequency regulation of the Spanish power system. To achieve this, several simulations were conducted using a BSP composed entirely of renewable energy, specifically, up to 30 wind farms. The output was then evaluated according to the new performance assessment framework established by the System Operator, which determines whether a BSP's performance should be economically penalised.

The studies demonstrated both the viability of this integration and the limitations that must be addressed.

The first algorithm is the Merit Order (MO) algorithm. The MO algorithm showed that wind energy can be fully utilised; however, this comes with the drawback of saturating certain units, while others are either solely responsible for regulation or remain at their minimum output throughout the simulation. These underutilised units could represent a poor return on investment, as their full capacity is not leveraged.

Moreover, having some wind farms saturated while others operate at minimum output can delay the system's response when those idle units are suddenly required to regulate. The performance of the BSP could then depend on the type of input signal received. This was particularly evident in the simulations with the *Sinusoidal Signal Near the Real Maximum Power* and *Sinusoidal Signal Near the Maximum and Minimum Power*, where the output lagged behind the setpoint due to the time required to ramp up idle turbines.

Additionally, output delays were observed when reaching the maximum available power (that will be usually quite different from the expected one). In such cases, the algorithm processes the deviation one cycle later, redistributing the ungenerated power among the remaining units.

Therefore, this algorithm is significantly affected by natural wind fluctuations, as most units operate at or near their maximum capacity. This introduces instability in the BSP's total performance. Furthermore, during periods with non-regulating units, the algorithm causes the majority of wind farms to become saturated, leaving insufficient capacity for the BSP to respond effectively to dynamic changes.

On the other hand, the MO Algorithm is not affected by the deadband or non-regulating units. Most of the units operate at their maximum output, and the units responsible for regulation have sufficient capacity to adjust power. Even if a few units are affected by the deadband, the overall performance of the BSP remains largely unaffected.

The second algorithm, the Proportional Regulation Band (PRB) algorithm, distributes power based on each unit's available regulation band. As a result, wind farms operate around the midpoint of their regulation ranges. No unit becomes saturated, allowing for faster responses to short-term changes and ensuring that all assets are effectively utilised. This collective responsiveness is a significant advantage compared to the MO Algorithm.

However, the PRB Algorithm is highly sensitive to the presence of non-regulating units and to deadbands. The deadband represents a critical challenge, as the proportional distribution often results in small changes that may fall within the deadband and therefore go unexecuted. Despite this, the algorithm manages to mitigate the issue in most cases, ensuring that no wind farm is assigned a setpoint it cannot fulfil.

An exception occurs when the setpoint power decreases toward the minimum limit. In these cases, units cannot be assigned setpoints below their technical minimum to avoid shutdowns, which could leave them operating within the deadband range. To avoid this, the algorithm applies larger adjustments to push units out of the deadband. However, this leads to noticeable fluctuations in the output power, caused by the step-like behaviour of wind farms jumping in and out of the deadband area.

Despite their respective limitations, both algorithms successfully met the objectives of the project. They effectively allocated the setpoint across the BSP's wind farms, achieving an

output that closely followed the system operator's setpoint with acceptable accuracy, mostly within the Active performance region of the evaluation framework even with the presence of measurement noise. This is particularly important because the algorithms were designed for real-world operation, where measurement noise is always present. In such conditions, performance is inevitably degraded, so achieving strong results without noise ensures they remain effective when noise is present. This was confirmed by the simulations with random noise, where both algorithms functioned correctly, with only minor performance degradation as expected. This demonstrates that both algorithms are capable of reliable operation under real-world conditions, where signals are frequently affected by noise.

Ultimately, this project confirms that renewable technologies, particularly wind farms, can be integrated into secondary frequency regulation. This enables operators and companies to select the most suitable algorithm based on their operational priorities and constraints.

Future work could focus on refining the algorithms further. For instance, the MO Algorithm could be enhanced to reduce the delay between input and output and the PRB Algorithm should be refined to eliminate the impact of non-regulating units on power distribution. In addition, the behaviour of both algorithms should be checked in a real-world system specially focusing in the presence of measurement noise. Depending on the results, the development of a filtering method should be necessary, though such filters may introduce latency, something that must be considered in future adaptations. Finally, the realism of the simulations could be improved by using actual system operator setpoint data and incorporating other renewable technologies beyond wind farms.

Chapter 7. REFERENCES

[1] 'Potencia instalada | Informes del sistema'. Accessed: Mar. 23, 2025. [Online]. Available: https://www.sistemaelectrico-ree.es/informe-del-sistema-electrico/potencia-instalada

[2] L. Y. Pao and K. E. Johnson, 'Control of Wind Turbines', *IEEE Control Systems Magazine*, vol. 31, no. 2, pp. 44–62, Apr. 2011, doi: 10.1109/MCS.2010.939962.

[3] K. De Vos and J. Driesen, 'Balancing management mechanisms for intermittent power sources — A case study for wind power in Belgium', in *2009 6th International Conference on the European Energy Market*, May 2009, pp. 1–6. doi: 10.1109/EEM.2009.5207190.

[4] A. Gonzalez-Garrido, A. Saez-de-Ibarra, H. Gaztanaga, A. Milo, and P. Eguia, 'Annual Optimized Bidding and Operation Strategy in Energy and Secondary Reserve Markets for Solar Plants With Storage Systems', *IEEE Trans. Power Syst.*, vol. 34, no. 6, pp. 5115–5124, Nov. 2019, doi: 10.1109/TPWRS.2018.2869626.

[5] B.-M. Hodge *et al.*, 'Wind Power Forecasting Error Distributions: An International Comparison: 11th International Workshop on Large-Scale Integration of Wind Power into Power Systems as well as on Transmission Networks for Offshore Wind Power Plants', *Proceedings of 11th International Workshop on Large-Scale Integration of Wind Power into Power Systems*, 2012.

[6] R. Bousso and R. Bousso, 'Don't blame renewables for Spain's power outage', *Reuters*, Apr. 30, 2025. Accessed: Apr. 30, 2025. [Online]. Available: https://www.reuters.com/business/energy/dont-blame-renewables-spains-power-outage-bousso-2025-04-30/

[7] 'How Spain powered back to life from unprecedented national blackout', BBC News. Accessed: Apr. 30, 2025. [Online]. Available: https://www.bbc.com/news/articles/c175ykvjxyeo

[8] C. Edmunds, S. Martín-Martínez, J. Browell, E. Gómez-Lázaro, and S. Galloway, 'On the participation of wind energy in response and reserve markets in Great Britain and Spain', *Renewable and Sustainable Energy Reviews*, vol. 115, p. 109360, Nov. 2019, doi: 10.1016/j.rser.2019.109360.

[9] C. A. Diaz, P. Gonzalez, Fco. A. Campos, and J. Villar, 'Spanish secondary reserve requirements, clearing and usage', in *11th International Conference on the European Energy Market (EEM14)*, Krakow, Poland: IEEE, May 2014, pp. 1–5. doi: 10.1109/EEM.2014.6861266.

[10] P. Li and R. Hu, 'Wind Turbines with DFIG Participate into Primary and Secondary Frequency Control by Suboptimal Power Tracking Method', 2018.

[11] N. de Frutos de la Torre, 'Mejora de un algoritmo de AGC para la integración de parques eólicos en regulación', 2023.

[12] T. Sow, O. Akhrif, A. F. Okou, A. O. Ba, and R. Gagnon, 'Control strategy insuring contribution of DFIG-Based wind turbines to primary and secondary frequency regulation', in *IECON 2011 - 37th Annual Conference of the IEEE Industrial Electronics Society*, Melbourne, Vic, Australia: IEEE, Nov. 2011, pp. 3123–3128. doi: 10.1109/IECON.2011.6119809.

[13] R. G. de Almeida and J. A. Pecas Lopes, 'Participation of Doubly Fed Induction Wind Generators in System Frequency Regulation', *IEEE Transactions on Power Systems*, vol. 22, no. 3, pp. 944–950, Aug. 2007, doi: 10.1109/TPWRS.2007.901096.

[14] M. Xu, Y. Jin, J. Ma, C. Wang, and P. Liu, 'Fuzzy Frequency Droop Control of DFIG Wind Turbine Generators Adapted to Continuous Changes in Wind Speeds', *IEEE Access*, vol. 11, pp. 115011–115024, 2023, doi: 10.1109/ACCESS.2023.3325245.

[15] Y.-K. Wu, C. Yin-Hsuan, D.-T. Trinh, T.-Y. Chen, and M.-H. Pham, 'A Complete Review of Frequency Regulation in Wind Turbines Considering Adaptive Droop/Inertia Hybrid Control', in *2025 IEEE/IAS 61st Industrial and Commercial Power Systems Technical Conference (I&CPS)*, May 2025, pp. 1–7. doi: 10.1109/ICPS64254.2025.11030345.

[16] A. Papakonstantinou, G. N. Psarros, and S. Papathanassiou, 'Power sharing and secondary frequency control for Greek island systems supplied by RES+storage hybrid stations and thermal generating plants', presented at the CIGRE Session 2024, Paris, France, Sep. 2024. Accessed: Feb. 22, 2025. [Online]. Available: https://www.researchgate.net/publication/383704492_Power_sharing_and_secondary_frequency_control_for_Greek_island_systems_supplied_by_RESstorage_hybrid_stations_and_thermal_generating_plants

[17] X. Wang, W. Bao, C. Zhang, and J. Chen, 'Coordination Between Wind Turbines and Energy Storage System for Frequency Regulation Participation', in *2023 International Conference on Power System Technology (PowerCon)*, Sep. 2023, pp. 1–5. doi: 10.1109/PowerCon58120.2023.10331557.

[18] Y. Fang, S. Zhao, E. Du, S. Li, and Z. Li, 'Coordinated Operation of Concentrating Solar Power Plant and Wind Farm for Frequency Regulation', *Journal of Modern Power Systems and Clean Energy*, vol. 9, no. 4, pp. 751–759, Jul. 2021, doi: 10.35833/MPCE.2021.000060.

[19] T. Ackermann, 'Wind Power in Power Systems', 2005.

[20] K. D. Vos, P. S. Perez, and J. Driesen, 'The Participation in Ancillary Services by High Capacity Wind Power Plants: Reserve Power'.

[21] A. Dreher, D. Jost, S. Otterson, and P. Hochloff, 'Pooled Frequency Restoration Reserve Provision by Wind Farms and Controllable Energy Units', in *2018 15th International Conference on the European Energy Market (EEM)*, Lodz, Poland: IEEE, Jun. 2018, pp. 1–6. doi: 10.1109/EEM.2018.8469902.

[22] I. Erlich and M. Wilch, 'Primary frequency control by wind turbines', in *IEEE PES General Meeting*, Jul. 2010, pp. 1–8. doi: 10.1109/PES.2010.5589911.

[23] J. L. Agüero, M. C. Beroqui, and F. Issouribehere, 'Grid frequency control. Secondary frequency control tuning taking into account distributed primary frequency control', in *IEEE PES General Meeting*, Jul. 2010, pp. 1–8. doi: 10.1109/PES.2010.5590004.

[24] I. Avramiotis-Falireas, P. Zolotarev, A. Ahmadi-Khatir, and M. Zima, 'Analysis and comparison of secondary frequency control reserve activation rules: Pro-rata vs. merit order', in *2014 Power Systems Computation Conference*, Aug. 2014, pp. 1–7. doi: 10.1109/PSCC.2014.7038293.

[25] 'INCREASING THE PENETRATION OF RENEWABLE ENERGY SOURCES IN THE DISTRIBUTION GRID BY DEVELOPING CONTROL STRATEGIES AND USING ANCILLARY SERVICES | FP7 | CORDIS | Commissione europea', CORDIS | European Commission. Accessed: Jun. 09, 2025. [Online]. Available: https://cordis.europa.eu/project/id/608998/reporting/it

[26] Ministerio de Industria, Energía y Turismo, *Resolución de 18 de diciembre de 2015, de la Secretaría de Estado de Energía, por la que se establecen los criterios para participar en los servicios de ajuste del sistema y se aprueban determinados procedimientos de pruebas y procedimientos de operación para su adaptación al Real Decreto 413/2014, de 6 de junio, por el que se regula la actividad de producción de energía eléctrica a partir de fuentes de energía renovables, cogeneración y residuos*, vol. BOE-A-2015-13875. 2015, pp. 119723–119944. Accessed: Jun. 09, 2025. [Online]. Available: https://www.boe.es/eli/es/res/2015/12/18/(2)

[27] E. Lobato Miguélez, I. Egido Cortés, L. Rouco Rodríguez, and G. López Camino, 'An overview of ancillary services in Spain', *Electric Power Systems Research*, vol. 78, no. 3, pp. 515–523, Mar. 2008, doi: 10.1016/j.epsr.2007.03.009.

[28] M. para la T. E. y el R. Demográfico, 'Procedimiento de Operación P.O. 7.2: Regulación secundaria'. Jun. 06, 2024. [Online]. Available: https://www.boe.es/boe/dias/2024/06/06/pdfs/BOE-A-2024-11535.pdf

[29] I. Egido Fernández-Bernal, F. ,. Rouco, L. ,. Porras, E. ,. Saiz-Chicharro, A., 'El control automático de la generación en el sistema peninsular español', *Anales de Mecánica y Electricidad*, vol. LXXXV, no. III, p. 31, May 2008.

[30] Viaintermedia.com, 'Estos son los quince mayores fabricantes de aerogeneradores del mundo', Energías Renovables, el periodismo de las energías limpias. Accessed: Feb. 25, 2025. [Online]. Available: https://www.energias-renovables.com/eolica/aqui-estan-los-diez-mayores-fabricantes-de-20200528

[31] 'Track Record | Vestas'. Accessed: Feb. 25, 2025. [Online]. Available: https://www.vestas.com/en/energy-solutions/track-record

[32] 'V100-2.0 MW®'. Accessed: Feb. 25, 2025. [Online]. Available: https://www.vestas.com/en/pages/backup-2-mw-platform/V100-2-0-MW

[33] 'Vestas V100/2000 - Fabricantes y aerogeneradores - Acceso en línea - The Wind Power'. Accessed: Feb. 25, 2025. [Online]. Available: https://www.thewindpower.net/turbine_es_779_vestas_v100-2000.php

ANEXO I. SUSTAINABLE DEVELOPMENT GOALS

This project aligns with the following Sustainable Development Goals:

1. **Affordable and Clean Energy (Goal 7)**

   The study conducted in this project focuses on the development of renewable energy. This type of energy is clean, as it harnesses natural sources such as wind, and its exploitation does not emit any pollutants (gases or waste). Moreover, it is accessible because it is inherently found in nature.

2. **Industry, Innovation and Infrastructure (Goal 9)**

   This project explores and develops new sources of secondary regulation for the Spanish Power System that have not yet been implemented, making it an innovative initiative. As a result, all industries in the country will be able to use more clean energy from renewable sources, promoting the growth of the renewable energy sector and involving the construction of new infrastructure.

3. **Sustainable Cities and Communities (Goal 11)**

   As explained in the previous point, the development of renewable energy leads to the creation of new infrastructure. Consequently, a greater share of the energy generated in the Spanish Power System will come from renewable sources. This will allow the energy demand to be met to a larger extent with clean and sustainable energy, thereby contributing to the development of sustainable cities and communities.

4. **Climate Action (Goal 13)**

   The project presents innovative and transformative ideas for the power system to address climate change. It promotes an energy source that does not emit greenhouse gases, helping to slow the rise in global temperatures and aligning with one of the necessary actions to combat climate change: transforming energy systems.